Developmental Biology

Tgfbr1 regulates lateral plate mesoderm and endoderm reorganization during the trunk to tail transition

Reviewed Preprint
v2 • December 17, 2024
Revised by authors

Reviewed Preprint
v1 • March 19, 2024

Anastasiia Lozovska, Ana Casaca, Ana Nóvoa, Ying-Yi Kuo, Arnon D Jurberg, Gabriel G Martins, Anna-Katerina Hadjantonakis, Moises Mallo

Instituto Gulbenkian de Ciência, Oeiras, Portugal • Gulbenkian Institute for Molecular Medicine, Lisboa, Portugal • Developmental Biology Program, Sloan Kettering Institute, Memorial Sloan Kettering Cancer Center, New York, USA

eLife Assessment

Morphological characteristics and phenotypes of mutations in key developmental genes suggest that head, trunk, and tail development are regulated by discernible modules. Gdf11 signalling plays a crucial role in orchestrating the transition from trunk to tail tissues in vertebrate embryos. This **important** study presents **convincing** evidence that Tgfbr1 acts upstream of Isl1 (a pivotal effector of Gdf11 signalling) and regulates blood vessels, the lateral plate mesoderm, and the endoderm associated with the trunk-to-tail transition. Together with the previous studies, this work identifies a key signal that acts as the pivot of the trunk-to-tail transition.

https://doi.org/10.7554/eLife.94290.2.sa2

Abstract

During the trunk to tail transition the mammalian embryo builds the outlets for the intestinal and urogenital tracts, lays down the primordia for the hindlimb and external genitalia, and switches from the epiblast/primitive streak to the tailbud as the driver of axial extension. Genetic and molecular data indicate that *Tgfbr1* is a key regulator of the trunk to tail transition. *Tgfbr1* has been shown to control the switch of the neuro mesodermal-competent cells from the epiblast to the chordo-neural hinge to generate the tail bud. We now show that Tgfbr1 signaling also controls the remodeling of the lateral plate mesoderm (LPM) and of the embryonic endoderm associated with the trunk to tail transition. In the absence of *Tgfbr1* the two LPM layers do not converge at the end of the trunk, extending instead as separate layers enclosing the celomic cavity until the caudal embryonic extremity, and failing to activate markers of primordia for the hindlimb and external genitalia. However, this extended LPM, does not exhibit the molecular signatures characteristic of this tissue in the trunk. The vascular remodeling involving the dorsal aorta and the umbilical artery leading to the connection between embryonic and extraembryonic circulation was also affected in the

Tgfbr1 mutant embryos. Similar alterations in the LPM and vascular system were also observed in *Isl1* null mutants, indicating that this factor acts in the regulatory cascade downstream of *Tgfbr1* in LPM-derived tissues. In addition, in the absence of *Tgfbr1* the embryonic endoderm fails to expand to form the endodermal cloaca and to extend posteriorly to generate the tail gut. We present evidence suggesting that the remodeling activity of *Tgfbr1* in the LPM and endoderm results from the control of the posterior primitive streak fate after its regression during the trunk to tail transition. Our data, together with previously reported observations, place *Tgfbr1* at the top of the regulatory processes controlling the trunk to tail transition.

Introduction

The transition from trunk to tail development is a complex process resulting in major changes in the general structure of the embryo, also involving a switch in the mechanisms regulating axial extension. Extension through the trunk is driven by axial progenitors located within the epiblast, that generate the spinal cord, the embryonic gut, and the different mesodermal compartments (Binagui-Casas et al., 2021; Cambray and Wilson, 2007; Henrique et al., 2015; Steventon and Martinez Arias, 2017; Tsakiridis and Wilson, 2015; Wilson et al., 2009; Wymeersch et al., 2021). At this stage, the caudal end of the mouse embryo is occupied by the allantois that will play an essential role in the connection between embryonic and extraembryonic structures (Arora and Papaioannou, 2012; Rodriguez and Downs, 2017). The transition to tail development is associated with changes in the global anatomy of the caudal end of the embryo, involving the progressive anterior relocation of the allantois along the ventral side of the embryo. During this process, the tail bud forms at the dorsal and posterior end of the embryo, and replaces the epiblast/primitive streak (PS) as the main driver of axial extension (Henrique et al., 2015; Wilson et al., 2009). Formation of the tail bud results from changes in the progenitors generating the neural and paraxial mesodermal structures, the so-called neuro-mesodermal competent (NMC) population, which relocates from the epiblast to the chordo-neural hinge (CNH) (Binagui-Casas et al., 2021; Cambray and Wilson, 2007; Wymeersch et al., 2021).

At this stage, the lateral plate mesoderm (LPM) also undergoes a major reorganization. This mesodermal compartment, generated by progenitors situated at the caudal region of the epiblast and PS (Wymeersch et al., 2021, 2019, 2016) is composed of two layers: a ventral splanchnopleure, which contributes to the formation of the various body organs, as well as their vascularization, and a lateral somatopleure involved in the formation of the body wall (Prummel et al., 2020). These two layers delimit the celomic cavity, which will hold the animal's internal organs. During allantois relocation, the two LPM layers converge towards the midline, ending the celomic cavity and marking the posterior border of the trunk. This remodeling of the caudal part of the embryo is associated with the induction of the hindlimbs from the somatopleure (Tickle, 2015), and the generation of the pericloacal mesenchyme, the primordium of the genital tuberculum (GT) (Cohn, 2011; Yamada et al., 2006), from the ventral lateral mesoderm (VLM) posterior to the allantois (Tschopp et al., 2014).

Concomitant with the reorganization of the embryonic mesoderm, the transition from trunk to tail development also involves major changes in the embryonic endoderm and in the vascularization that will connect embryonic and extraembryonic structures. When the allantois relocates, the embryonic endoderm, whose posterior end reaches the base of the allantois, forms a cavity that will originate the cloaca, an endodermal expansion that becomes the common end of the excretory, intestinal, and genital tracts (Huang et al., 2016; Matsumaru et al., 2015). The pronephric ducts, derivatives of the intermediate mesoderm (IM) located medially to the splanchnic and somatic LPM layers, later merge with the cloaca to engage in the development of the urogenital system (Davidson, 2008). In the mouse embryo, the embryonic endoderm then expands further caudally to generate the tail gut, a transient structure with unknown function.

The region of the posterior visceral (extra-embryonic) endoderm abutting the allantois is thought to facilitate the invagination and growth of the embryonic endoderm (Rodriguez and Downs, 2017) and contribute to the hindgut epithelium (Kwon et al., 2008; Nowotschin et al., 2019).

The major blood vessels also become reorganized with the relocation of the allantois. The caudal end of the paired dorsal aortae (DA) merge and connect with the umbilical artery generated within the allantois (Arora and Papaioannou, 2012; Downs and Rodriguez, 2020). As the allantois move forward, the caudal end of the DA bends to form the recurved dorsal aorta (rDA). It is thought that this process requires the generation of a vessel of confluence from the caudal end of the PS abutting the allantois, which will constitute a major part of the rDA (Downs and Rodriguez, 2020; Rodriguez and Downs, 2017). Reorganization of the DA/umbilical artery connection will generate the blood vessels linking the embryo with the placenta and will also generate the arteries that will provide irrigation to the hindlimbs.

Molecular and genetic data indicate that Gdf11 signaling is an integral component of the gene regulatory network controlling the trunk to tail transition (Aires et al., 2019; Jurberg et al., 2013; Matsubara et al., 2017; McPherron et al., 2009, 1999). Gdf11 activity is predominantly mediated by transforming grow factor β receptor 1 (Tgfbr1) (also known as Alk5) (Andersson et al., 2006). Indeed, premature expression of a constitutively active form of Tgfbr1 promotes early execution of the trunk to tail transition program (Jurberg et al., 2013). In addition, *Tgfbr1* is required to trigger formation of the tail bud by promoting, together with *Snai1*, an incomplete epithelial to mesenchymal transformation (EMT) in the NMC population within the epiblast (Dias et al., 2020). In the present study we show that, in addition to the lack of molecular signals for the induction of the hindlimbs and the GT, the LPM of *Tgfbr1* null mutants fail to converge leading to the posterior extension of the celomic cavity. In addition, the mutants fail to generate a cloacal cavity and to extend the endodermal tube to form the tail gut. Also, the connection between the embryonic and extraembryonic vascular systems fails to undergo normal reorganization, resulting in the expansion of the paired dorsal aorta to reach the caudal end of the embryo. We also provide evidence indicating that *Isl1* is the key functional downstream target of *Tgfbr1* for the reorganization of the LPM and vascular tissues during the trunk to tail transition, acting on the posterior PS/allantois. *Isl1* controls PS fate during its regression and regulates the establishment of the embryonic-extraembryonic connection during the ventral relocation of the allantois. Taken together, our findings indicate that *Tgfbr1* is a master regulator of the trunk to tail transition.

Materials and methods

Mouse lines and embryos

The *Tgfbr1*$^{+/-}$ (Dias et al., 2020), Alf-GFP (Kwon et al., 2008), ROSA26-R-gal (Soriano, 1999), ROSA26-R-EYFP (Srinivas et al., 2001) and *Isl1-cre* (Srinivas et al., 2001) used in this work have been previously described. T-str-creERT was generated by cloning the creERT cDNA, containing the SV40 polyadenylation signal obtained from the *Cdx2-creERT* construct (Jurberg et al., 2013), under the control of the PS enhancer of the Brachyury (*Tbxt*) gene (Clements et al., 1996). The construct was used to generate transgenic animals by pronuclear microinjection according to standard protocols (Hogan et al., 1994). Mutant and transgenic lines were genotyped from ear or digit biopsies incubated in 50 µL of PBND buffer (50 mM KCl, 10 mM Tris-HCl, pH 8.3, 2.5 mM $MgCl_2$, 0.1 mg/mL gelatin, 0.45% NP40, 0.45% Tween 20) supplemented with 100 µg/mL of proteinase K at 55°C overnight. Samples were incubated at 95°C for 15 minutes to heat-deactivate proteinase K. 1 µL of genomic DNA was used in PCR reaction with the relevant primers specified in **Table 1**.

Genotyping primers		
Tgfbr1 mutant allele	Forward	CTACTGTGTTTCAAATGGGAGGGC
	Reverse	GGCCTGTCGGATCCTATCATC
Tgfbr1 wild type allele	Forward	CTACTGTGTTTCAAATGGGAGGGC
	Reverse	ACATACAAATGGCCTGTCTCG
Isl1 mutant allele	Forward	GCCACTATTTGCCACCTAGC
	Reverse	AGGCAAATTTTGGTGTACGG
Isl1 wild type allele	Forward	GCCACTATTTGCCACCTAGC
	Reverse	CAAATCCAAAGAGCCCTGTC
Cre recombinase	Forward	CGAGTGATGAGGTTCGCAAG
	Reverse	CCTGATCCTGGCAATTTCGGCT

Table 1.

Tgfbr1 null and *Isl1* null embryos were generated from intercrosses between *Tgfbr1*$^{+/-}$ and *Isl1-cre*$^{+/cre}$mice, respectively. Embryos obtained from heterozygous crossings were genotyped from their yolk sacs. Yolk sacs were collected to 50 µL of lysis buffer (50 mM KCl, 10 mM Tris-HCl, pH8.3, 2 mM $MgCl_2$, 0.45% Tween-20, 0.45% NP40) supplemented with 100 µg/mL of proteinase K and incubated at 55°C overnight. Samples were heat-deactivated as described above. PCR was performed using 1 µL of genomic DNA using the primers specified in **Table 1**.

Whole mount in situ hybridization and sectioning

Embryos were fixed in 4% paraformaldehyde in PBS (PFA) overnight, then dehydrated through a 25%, 50% and 75% series of methanol in PBT (PBS, 0,1% Tween 20), then incubated in 100% methanol. Embryos were then rehydrated through a reverse methanol/PBT series and incubated three times in PBT for at least 5 min each at room temperature. Embryos were then bleached for 1 hour in 6% hydrogen peroxide in PBT and permeabilized in 10 µg/mL of proteinase K in PBT for a time period that depended on the embryo size. The reaction was then quenched with a 2 mg/mL solution of glycine in PBT, washed twice in PBT and postfixed in a 4% PFA and 0,2% glutaraldehyde mix for 20 minutes, followed by two washes in PBT. Hybridization was performed at 65°C overnight in hybridization solution (50% formamide, 1.3 x SSC pH 5.5 [20 x SSC is 3M NaCl, 300 mM sodium citrate], 5 mM EDTA, 0.2 % Tween 20, 50 µg/mL yeast tRNA, 100 µg/mL heparin) containing the relevant digoxigenin-labelled antisense RNA probes. RNA probes were *in vitro* transcribed from the linearized vector for 3 hours at 37°C with the corresponding RNA polymerase and DIG RNA Labeling Mix (Roche #11277073910). The reaction product was verified in 0,8% agarose gel and diluted in hybridization solution for further use. After hybridization, embryos were washed twice at 65°C with hybridization solution without tRNA, heparin, and the RNA probe and then in a 1:1 mix of hybridization solution and TBST (25 mM Tris-HCl, pH 8.0, 140 mM NaCl, 2.7 mM KCl, 0.1% Tween 20) for 30 min at 65°C. Embryos were then washed three times with TBST at room temperature, equilibrated in MABT (100 mM maleic acid, 150 mM NaCl, 0.1 % Tween-20, pH 7.5) and blocked in MABT blocking buffer [MABT containing 1% blocking reagent (Roche #11096176001)] with 10% sheep serum for 2.5 hours at room temperature. Embryos were then incubated overnight at 4°C with a 1:2000 dilution of alkaline phosphatase-conjugated anti-digoxigenin antibody (Roche #11093274910) in MABT blocking buffer with 1% sheep serum. After extensive washes with MABT at room temperature, embryos were equilibrated in NTMT buffer (100 mM Tris HCl, pH 9.5, 50 mM $MgCl_2$, 100 mM NaCl, 0.1% Tween-20) and developed with a 1:50 dilution of NBT/BCIP solution (Roche #11681451001) in NTMT at room temperature in the dark. Stained embryos were mounted in a 0,45% gelatin, 27% bovine serum albumin (BSA), 18% sucrose mix, jellified with 1,75% glutaraldehyde and sectioned at 35 µm on a Leica Vibratome VT 1000 S.

Whole mount immunofluorescence and image processing

Embryos were fixed in 4% PFA on ice for 2 hours and then dehydrated through a 25%, 50%, 75% methanol/PBST (PBS, 0,1% Triton-X 100) series followed by 100% methanol. Embryos were then rehydrated through a reverse methanol PBST series, washed with PBST and permeabilized in 0,5% Triton-X 100 in PBS for 1 hour and incubated in 1M glycine in PBST for 30 minutes to reduce unspecific binding. After several washes in PBST embryos were blocked in 1% BSA, 3% donkey serum in PBST at 4°C overnight. Embryos were then incubated for 72 hours at 4°C with the following dilutions of the primary antibodies in blocking buffer: Pecam1 1:50 (ab28364, Abcam), Keratin 8 1:100 (Troma1, developed by Dr Brulet and Dr Kemler, obtained from the NICHD Developmental Studies Hybridoma Bank maintained by the University of Iowa). Secondary antibodies were diluted 1:1000 in blocking buffer and embryos incubated for 48 hours at 4°C. After extensive washes in PBST embryos were stained with a 1:10000 DAPI dilution in PSBT at 4°C overnight. Embryos were then mounted on a depression slide with RapiClear 1.49 clearing reagent (SunJin lab). Embryos were imaged on a Prairie Multiphoton microscope using an Olympus 20X 1.0 NA W objective. Stacks were then digitally stitched in Fiji using the Grid/Collection stitching plugin. After removing the outliers, tissues were segmented using Amira Software.

Analysis of the contribution of the visceral endoderm to the embryonic gut

E7.5 embryos were fixed for 20 min in 4% PFA at room temperature, washed three times in PBST, and then counterstained in 5 µg/ml Hoechst and 5 U/ml phalloidin before imaging. E8.5 embryos were permeabilized in 0.5% Triton-X100 in PBS for 20 min, washed three times in PBST and incubated in blocking buffer containing 5% donkey serum (Jackson Labs) and 1% BSA in PBST for 1 h at 4 °C. Embryos were then incubated overnight at 4 °C with Epcam (cat#118202, Biolegend) (1:100) and GFP (GFP-1020, Aveslabs) (1:500) in blocking buffer. After 3 washes in PBST, embryos were incubated with secondary antibody (1:500) overnight at 4 °C, and then washed again 3 times in PBST and counterstained in 5 µg/ml Hoechst. For E9.5 and E10.5 embryos, samples were fixed for 1 h in 4% PFA at room temperature, washed three times in PBS, then dehydrated through a 25%, 50%, 75% methanol/H_2O series followed by 100% methanol. Embryos were stained with antibodies against Epcam (1:100) and GFP (1:500) using the iDISCO+ tissue clearing protocol as previously described (Renier et al., 2014), (updated at *https://idisco.info/*). E7.5 embryos were mounted in PBS and imaged on a Zeiss LSM880 using a Plan-Apo 20×/NA0.8 M27 objective. E8.5 embryos were mounted in FocusClear clearing reagent and imaged on a Zeiss LSM 880 using a Plan-Apo 20×/NA0.8 M27 objective. E9.5 embryos were mounted in dibenzyl ether (DBE) and imaged on a Zeiss LSM 880 using a Plan-Apo 20×/NA0.8 M27 objective and an EC Plan-NEOFLUAR 10×/NA0.3 objective. E10.5 embryos were imaged on a Luxendo MuVi SPIM light-sheet microscope using a Nikon Plan-Apo 10×/NA0.8 Glyc objective. Raw image data were processed in ZEN (Zeiss, *https://www.zeiss.com/microscopy/us/products/microscope-software/zen.html*), Luxendo Image Processor, or Imaris (Bitplane, *http://www.bitplane.com/*) software.

Ex vivo culture with DiI labelling

E9.5 embryos were dissected out in ice cold media [DMEM (Gibco®, Life Technologies)/15% FBS/11mM HEPES (Sigma)]. Stock DiI solution was prepared by dissolving aliquot of powdered CellTracker^{TM} CM-DiI (Life technologies, C7000) in 10 µl of 96% ethanol. Working labeling solution was a 1:10 dilution of the stock solution in 0.3 M sucrose (Sigma). Embryos were injected with labeling solution in the ventral tailbud by mouth pipetting using a glass capillary and collected individually in a 24 well-plate on ice. Injected embryos were first imaged on SteREO Lumar.V12, Zeiss and then cultured for 20 h at 37°C in a rotator bottle culture apparatus (B.T.C. Engineering, Milton, Cambridge, UK) at 37°C, in a 65% O_2 atmosphere. Each embryo was cultured individually in a tube with 1.5 mL of DMEM/F-12, GlutaMAX™ (Gibco®, Life Technologies, 31331-028) containing 15%FBS, 11mM HEPES (Sigma) and supplemented with a penicillin/ streptomycin mixture. Cultured embryos were washed with PBS, imaged on SteREO Lumar.V12, Zeiss and fixed in 4% PFA for 1 h at room temperature. Next, embryos were permeabilized with 0,3% Tween in PBS for 1 h at room temperature. Nuclei were stained with a 1:5000 solution of DAPI in PBS for 16 h at 4°C with rotation. Embryos were then washed in PBS, mounted on depression slides, and cleared with RapiClear 1.49 clearing reagent (SunJin lab). Imaging was done on a Prairie Multiphoton microscope using an Olympus 20X 1.0 NA W objective.

Reporter tracing with T-str-creERT transgenics

Pregnant females from T-str-creERT and either ROSA26-R-βgal or ROSA26-R-YFP intercrosses were treated with tamoxifen (200 µl of a 1 mg/ml solution in corn oil) by oral gavage at different times from E7.5 to E8.5 and harvested at E9.5 or E10.5. When the ROSA26-R-YFP reporter was used, embryos were dissected on PBS and observed with SteREO Lumar.V12, Zeiss. When the ROSA26-R-βgal reporter was used embryos were fixed with 4% PFA at 4°C for 30 min, then washed three times in PBS containing 0.02% Tween 20 for 10 min each at room temperature and developed with 0.4 mg/ml X-gal in 5 mM $K_3Fe(CN)_6$, 5 mM $K_4Fe(CN)_6.3H_2O$, 2 mM $MgCl_2$, 0.02% NP40, 0.02% Tween 20, in PBS for several hours at 37°C in the dark. The reaction was stopped with wash buffer, fixed with 4% PFA overnight and sectioned as described for the whole mount in situ-stained embryos.

To test the time required to observe reporter activity upon tamoxifen treatment, pregnant females from T-str-creERT and ROSA26-R-YFP intercrosses were treated with a single tamoxifen dose and embryos recovered after 6, 8 or 10 hours after treatment and evaluated for YFP signal.

Results

Tgfbr1 is a key modulator of the caudal trunk mesoderm differentiation

We previously showed that *Tgfbr1* null mutant embryos fail to activate markers labeling the hindlimb and GT primordia (the VLM) (Dias et al., 2020). We now assessed the defects of the *Tgfbr1* mutants at the axial level at which these genes become active in wild type embryos. Transverse sections through this area indicated abnormal morphology of the LPM (**Fig. 1**). In wild type embryos, the somatic and splanchnic LPM layers converge at the posterior region of the trunk at both sides of the developing endoderm at E9.5, ending the celomic cavity. In *Tgfbr1* mutant embryos, however, the two LPM layers, and, consequently, the coelomic cavity, continued extending from the trunk region of the embryo until its posterior end (**Fig. 1 b',d'**). Despite this apparent extension of the trunk LPM into the prospective hindlimb and VLM regions, molecular analyses suggested that the LPM properties in this area differed from those observed in the trunk. This was best illustrated by the expression of *Irx3* and *Foxf1*, somatic and splanchnic LPM markers, respectively (Funayama et al., 1999; Mahlapuu et al., 2001). Both markers were expressed following normal patterns in the trunk of *Tgfbr1*$^{-/-}$ embryos (**Fig. 1Aa, Bb, Cc, Dd**). However, in contrast to wild type controls, in *Tgfbr1* null mutant embryos these markers were not down regulated at the level of the trunk to tail transition, being *Foxf1* even clearly up regulated in this embryonic region (**Fig.1B,D**). In addition, their expression was no longer restricted to their respective LPM layers, and instead expanded to encompass the entire mesodermal tissue surrounding the celomic cavity. This feature was more clearly observed for *Foxf1* (**Fig. 1Dd'**). The expression pattern of the IM marker *Pax2* at E10.5 revealed that the pronephric ducts also extended into the posterior end of the embryo instead of merging with the cloaca (Supplementary Fig.1c,c',d"). Furthermore, pronephric ducts were bifurcated in the posterior embryonic end in some mutant embryos (2/4) (Supplementary Fig.1D-d").

Another major mesodermal derivative affected by the absence of *Tgfbr1* was the main vascular tree, particularly the region connecting embryonic and extraembryonic circulation. The four orifices surrounding the hindgut in E9.5 embryos observed in transverse sections, and diagnostic of the recurved dorsal aorta (rDA) (Zakin et al., 2005), were not detected in *Tgfbr1* mutants, in which only a single expanded vessel was visible on each side of the gut tube (**Fig. 1Aa',Bb',Cc',Dd'**). Pecam1-aided 3D reconstruction of the main blood vessels revealed that the DA of *Tgfbr1* mutant embryos was elongated posteriorly, reaching the tip of the gut tube. The posterior portion of the DA formed a vessel of enlarged diameter, as observed in the histological sections, that contrasts with the curvature characteristic of the rDA of wild type embryos (**Fig. 2**). The DA of the *Tgfbr1* mutants still merged with the umbilical artery, although following patterns different to those observed in control embryos. For instance, while in wild type embryos the paired rDAs remained as two independent vessels, merging just before their connection with the umbilical artery (**Fig. 2b**), the two paired arteries of *Tgfbr1*$^{-/-}$ embryos were fused along most of their path ventral to the endodermal tube, from the posterior embryonic tip to the umbilical artery. In addition, the allantois appeared to protrude perpendicularly to the embryo instead of following its curvature, as observed in wild type embryos (**Fig. 2d**).

Together, the above observations indicate that in the absence of *Tgfbr1* the mesodermal tissues derived from the lateral mesoderm fail to execute the normal differentiation routes associated with the trunk to tail transition.

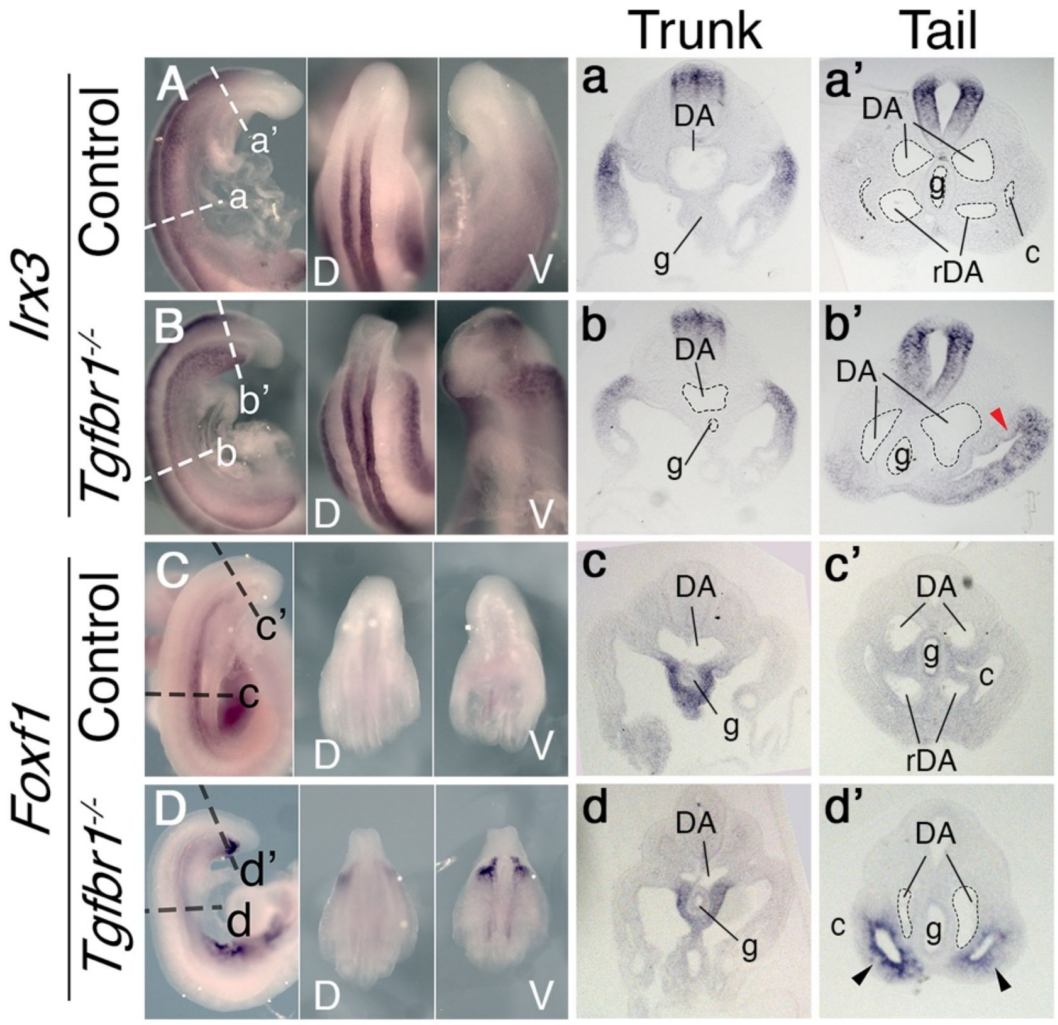

Figure 1.

In situ hybridization showing expression patterns of the main mesodermal markers.

A – d'. Expression of somatic LPM marker *Irx3* (A, B) and splanchnic LPM marker *Foxf1* (C, D) in control (A, C) and *Tgfbr1*$^{-/-}$ (B, D) E9.5 embryos. Next to the images of the whole mount embryos shown transversal sections through trunk (a – d) and tail (a' – d') regions. Red arrowhead indicates ectopic expression of *Irx3* in splanchnic LPM, black arrowhead – ectopic expression of *Foxf1* in somatic LPM. c – coelomic cavity, cl – cloaca, DA – dorsal aorta, g – gut, g – gut, rDA – recurved dorsal aorta, V – ventral, D – dorsal.

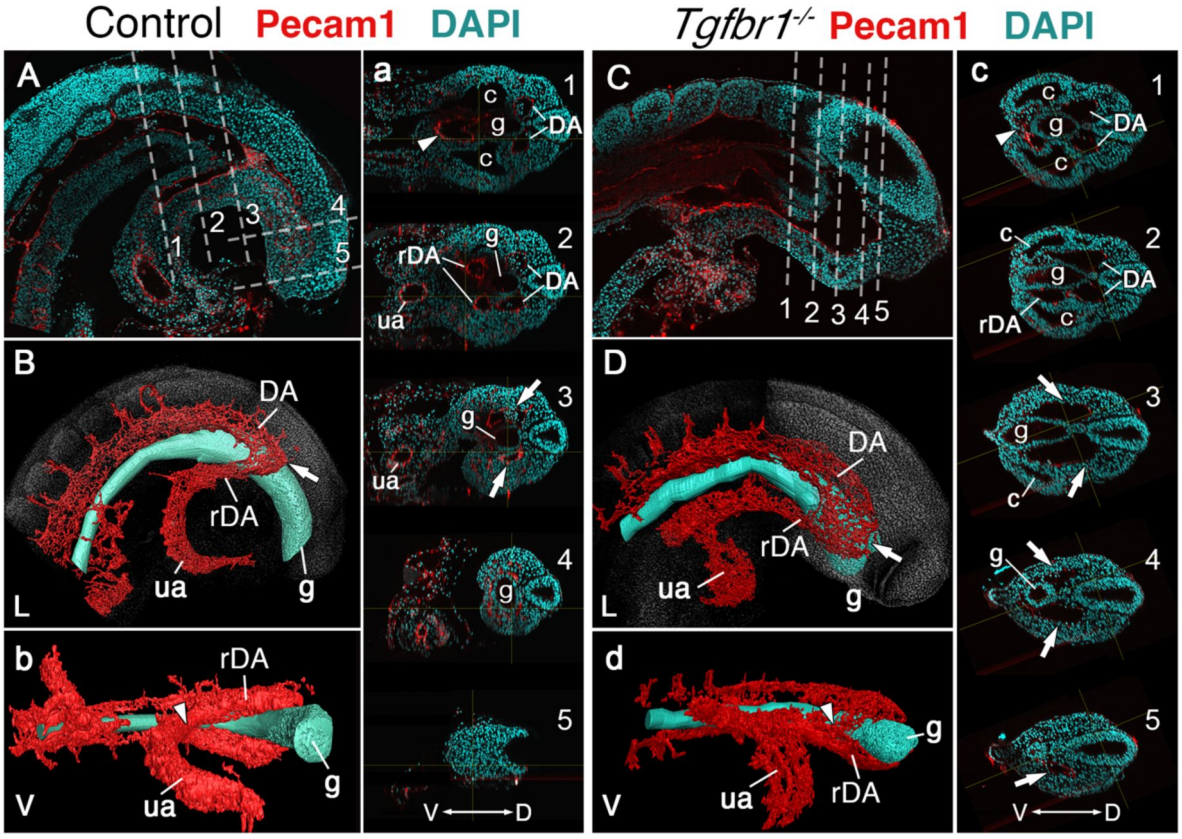

Figure 2.

Main vascular tree of the *Tgfr1*$^{-/-}$ embryos.

A, a, C, c. Wholemount immunostaining for Pecam1 (red) labelling endothelial cells in E9.5 control (A, a) and mutant (C, c) embryos. Nuclei shown in cyan. Transversal sections through regions marked by the dashed lines in A and C are shown in (a1-5) and (c1-5). **B, b, D, d.** 3D reconstruction of the main vascular tree (red) and the gut (cyan) of the immunostaining shown in (A, a, C, c). Connection between the umbilical artery (ua) and recurved dorsal aortae (rDA) is marked by the arrowhead. Turn of dorsal aortae (DA) where it is connected to rDA is labelled by the arrow. In the mutant this region is enlarged while rDA is short (compare A, a3 and B to C, c2-5, and D). D – dorsal, L – lateral, V – ventral, c – coelomic cavity, g – gut.

Possible involvement of the posterior PS as mediator of Tgfbr1 activity

Splanchnic *Foxf1* expression depends on endodermal Shh activity (Astorga and Carlsson, 2007; Tsiairis and McMahon, 2009). The *Foxf1* expression observed in the lateral layer of the expanded LPM of *Tgfbr1* mutant embryos is separated from the endoderm by the celomic cavity, suggesting that it is likely to have a Shh-independent origin. Such *Foxf1* expression has been detected in the posterior PS/allantois of E8.5 embryos (Astorga and Carlsson, 2007; Tsiairis and McMahon, 2009), where it plays a role in vasculogenesis (Astorga and Carlsson, 2007). Reorganization of the vascular system to connect the embryonic and extraembryonic circulation occurs within the emergent VLM as the allantois becomes displaced anteriorly during the trunk to tail transition (Downs and Rodriguez, 2020; Rodriguez and Downs, 2017). From a functional perspective, *Foxf1* expression in the VLM is likely to derive from its expression domain in the posterior PS/allantois (Supplementary Fig. 2). *Foxf1* expression in the posterior PS/allantois is not affected by the absence of *Tgfbr1* (**Fig. 3A,B**), consistent with the apparent dispensability of *Tgfbr1* activity in axial tissues before the transition to tail development. Given the absence of VLM in *Tgfbr1*$^{-/-}$embryos, the *Foxf1*-positive cells in the extended LPM might represent the derivatives of posterior PS/allantois cells that failed to enter their normal fates, which instead become intermingled with LPM cells extending from the trunk. Indeed, the abnormal development of the posterior aortae in *Tgfbr1* mutant embryos might result from compromised development of the *Foxf1*-positive posterior PS/allantois.

To assess whether the PS contributes to the prospective pericloacal region, we generated a transgenic line (*T-str-creERT*) expressing the tamoxifen-inducible cre recombinase in the PS under the control of an enhancer of *Brachyury* (currently known as *Tbxt*)(Clements et al., 1996) and inducing cre-mediated ROSA26-derived reporter expression (Soriano, 1999; Srinivas et al., 2001) (Supplementary Fig. 3). Tamoxifen administration at E8.0, which activates cre activity within the 10-12 hours corresponding to E8.5 (Supplementary Fig. 4), thus coincident with the start of the trunk to tail transition, resulted in labeling of the VLM of E9.5 embryos, and of the pericloacal mesoderm at E10.0 (**Fig. 3c**). Although this experiment does not allow regional sub localization within the PS, it is consistent with the *Foxf1*-positive posterior PS/allantois being a functional target of *Tgfbr1* activity in the LPM during the trunk to tail transition.

Isl1 mediates *Tgfbr1* activity in the lateral mesoderm

Reporter, gain and loss of function experiments suggested that *Isl1* might be functioning downstream of Tgfbr1 signaling in the LPM during the trunk to tail transition (Dias et al., 2020; Jurberg et al., 2013). It has been shown that *Isl1* first becomes activated in axial tissues at the PS/allantois junction, just prior to the transition to tail development (Cai et al., 2003; Wymeersch et al., 2019), and Isl1-positive cells later contribute to the VLM, the hindlimbs and GT (Yang et al., 2006). Analysis of the role of *Isl1* during the trunk to tail transition might thus provide an independent test of the functional relevance of the posterior PS/allantois for *Tgfbr1* activity in the LPM during the transition. We generated *Isl1* null mutant embryos using the null allele resulting from the insertion of the cre recombinase replacing the *Isl1* gene in the *Isl1-cre* strain (Srinivas et al., 2001). *Isl1* null embryos were embryonic lethal between E9.5 and E10.5, showing malformations in different embryonic structures. Regarding axial development, *Isl1* mutants halted their growth around the stage of the trunk to tail transition, as estimated by the number of somites generated (**Fig. 4D,E,F,I,J**), thus reminiscent of the *Tgfbr1* mutant phenotype. However, in contrast to *Tgfbr1* mutants, *Isl1* mutants generated a structure resembling the tail bud which expressed *Sox2* and *Tbxt* in domains comparable to wild type embryos (**Fig.4A,B,D,E**). The presence of a tail bud in *Isl1* mutants indicates that this gene might not be involved in the activity of the NMC cells, as suggested by its expression pattern (Cai et al., 2003). However, we observed major morphological and molecular alterations in the region corresponding to the LPM. Interestingly, some of those alterations are comparable to the defects observed in *Tgfbr1* mutants.

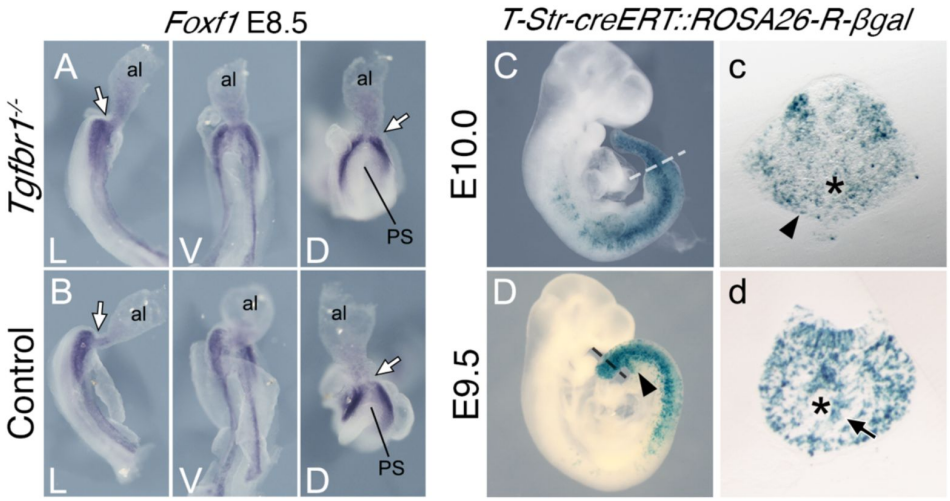

Figure 3.

Posterior primitive streak contributes to the pericloacal mesenchyme and gut endoderm.

A, B. Whole mount in situ hybridization showing expression of *Foxf1* in E8.5 *Tgfbr1*$^{-/-}$ (A) and control (B) embryos. al – allantois, g – gut, PS – primitive streak. L – lateral view, V – ventral view, D – dorsal view. While arrow indicates PS/allantois junction. **C-d.** β-galactosidase cell tracing showing descendance of the primitive streak in the E10.0 (C, c) and E9.5 (D, d) embryos. c and d show transversal sections through regions marked by the dashed lines in C and D. Black arrowhead shows β-galactosidase staining in the pericloacal mesenchyme. Black arrow in d shows β-galactosidase^{+} cells in the tail gut endoderm. The asterisk in c indicates the cloaca. The asterisk in d indicates the tail gut.

The two layers of the lateral mesoderm, as well as the celomic cavity, extended to the posterior extremity of the embryo (**Fig. 4H,h',h''**). *Foxf1* expression was also upregulated in the posterior of the embryo, showing a spatial distribution that starts at the dorsal border between the splanchnic and somatic LPM layers, extending to fully cover the somatic lateral mesoderm at more posterior embryonic regions (**Fig. 4h',h''**). In addition, the dorsal aortae were expanded into two globular vessels on either side of the gut tube reaching the caudal embryonic end where they merged ventrally (**Figs 4h,h', 5C,c,D,d**). The connection between umbilical artery and the expanded DAs was highly disorganized (**Fig. 5D**). Together, these observations indicate that *Isl1* acts downstream of *Tgfbr1* to regulate the processes associated with the trunk to tail transition in the LPM, including the main vascular system, and are consistent with the *Foxf1*-positive area of the posterior PS/allantois being a functional target of Tgfbr1 signaling to reorganize the LPM during the trunk to tail transition.

Molecular analyses showed that *Tbx4* was not expressed in the posterior part of *Isl1* mutants (**Fig. 4I,I',J,J'**), indicating that *Tbx4* is downstream of *Isl1* in the regulatory network controlling the hindlimb/external genitalia, consistent with previous observations using a conditional mutant for *Isl1* (Itou et al., 2012; Kawakami et al., 2011).

Proper development of the embryonic endoderm requires *Tgfbr1*

Analysis of transverse sections of the *Tgfbr1* mutant embryos suggested abnormal morphogenesis of the gut tube. Consistent with this, expression of two endodermal markers, *Foxa2* and *Shh* (Ang et al., 1993; Echelard et al., 1993) at E9.5 showed abnormal morphology at the posterior end of the gut tube (**Fig. 6A,a,B,b** and Supplementary Fig. 5). This abnormal morphology was clearer in mutant embryos immunostained with the epithelial marker Keratin 8 (Runck et al., 2014), where it was observed that the endodermal tube finished contacting the ventral ectoderm forming a structure reminiscent of the cloacal membrane (**Fig. 6C,D**). Also, in contrast with what was observed in wild type controls, *Tgfbr1*$^{-/-}$ embryos lacked the endodermal widening characteristic of the developing cloaca and failed to extend the endodermal tube caudal to the cloacal membrane to form the tail gut (**Fig. 6C,D**). Remarkably, expression of the endodermal marker *Apela* (Hassan et al., 2010) followed abnormal patterns in *Tgfbr1* mutants. Contrary to wild type embryos, in which the tail endodermal tube was strongly positive for *Apela* (**Fig. 6E,e,F,f**), in the *Tgfbr1* mutants most of the endodermal tube was negative for this marker, its expression being observed only in a few cells in the dorsal part of the gut tube (**Fig. 6E',e',F',f'**). Surprisingly, *Apela* positive cells were found mixed with the cells of the expanded LPM (**Fig. 6E',F'**), suggesting that endodermal progenitors were produced but misrouted, failing to enter the gut tube. Consistently with the endodermal origin of the *Apela* positive cells, we observed Keratin 8 staining scattered within the extended LPM of the mutant embryos (**Fig. 6c,d**).

It has been shown that the visceral endoderm contributes to the formation of the embryonic gut, with the hindgut being particularly populated by this extraembryonic tissue (Kwon et al., 2008). To understand whether the absence of cloacal and tailgut structures in the *Tgfbr1* mutants resulted from the inability of the posterior visceral endoderm cells to become incorporated into the embryonic definitive endoderm, becoming instead mixed with the mis-patterned LPM cells, we introduced the visceral endoderm reporter *Afp-GFP* transgene (Kwon et al., 2008) into the *Tgfbr1* mutant background. Analysis of E7.5 *Afp-GFP*$^{+/0}$*:Tgfbr1*$^{-/-}$ embryos indicated that the dispersal of visceral endodermal cells was not affected by the absence of *Tgfbr1* (Supplementary Fig. 6). In addition, Afp-GFP positive visceral endoderm cells were observed in the embryonic endoderm of *Tgfbr1* mutant embryos at E8.5, in a distribution comparable to wild type embryos (**Fig. 7A,A',B,B'**). At later stages of development, however, when embryos engage in tail development, distinct distributions were observed in the wild type and mutant embryos. Both at E9.5 and E10.5, the entire endodermal tube of *Tgfbr1*$^{-/-}$embryos contained GFP positive cells, also showing the premature end at the ventral surface of the embryo and the absence of further posterior extension to form the tail gut (**Fig. 7D-D'',F,F'**). Importantly, we did not observe Afp-GFP signal mixed with the extended LPM (**Fig. 7F'',F'''**). These data thus indicate that the

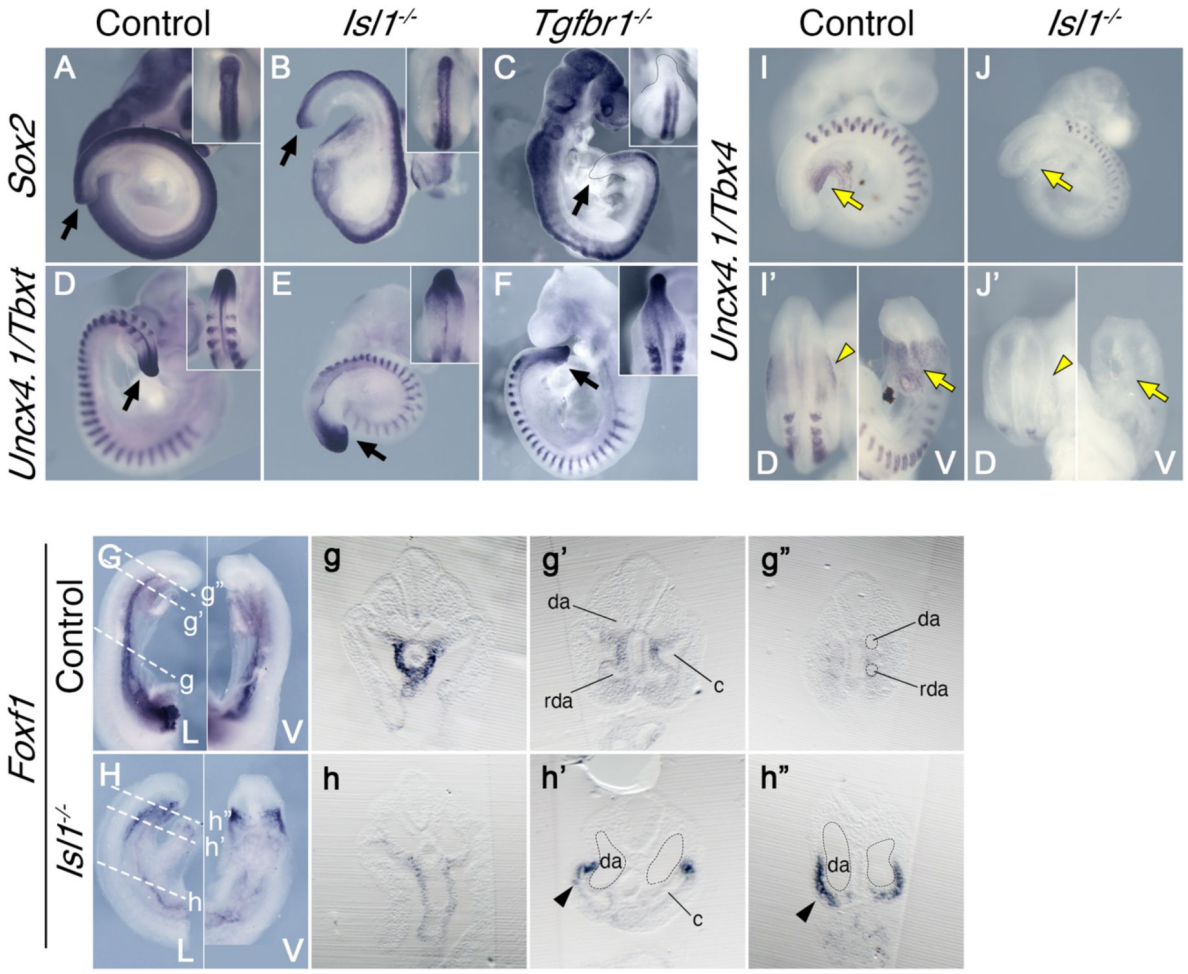

Figure 4.

Effects of *Tgfbr1* in the LPM, but not in the tail bud, are mediated by *Isl1*.

A-F". Whole mount *in situ* hybridization showing expression of *Sox2* (A-C) and *Uncx4.1/Tbxt* (D-F) in the E9.5 control (A, D), *Isl1*$^{-/-}$ (B, E), and *Tgfbr1*$^{-/-}$ (C, F) embryos. *Isl1*$^{-/-}$ embryos form tail bud (black arrows), unlike *Tgfbr1*$^{-/-}$ embryos. Insets in the right top corners show dorsal view of the tail bud region. **G, h".** Whole mount *in situ* hybridization showing expression of *Foxf1* in the E9.5 control (G) and *Isl1*$^{-/-}$ (H) embryos. g-g" and h-h" show transversal sections through the regions marked by the dashed line in G and H. *Foxf1* is ectopically expressed in the splanchnopleure of the posterior region of the *Isl1*$^{-/-}$ (black arrowhead in h' and h"). **I-J'.** Whole mount *in situ* hybridization showing expression of *Uncx4.1/Tbx4* in E9,5 control (I, I') and *Isl1*$^{-/-}$(J, J') embryos. *Tbx4* is not expressed in pericloacal mesenchyme (yellow arow) and hindlimb buds (yellow arrowheads) of *Isl1*$^{-/-}$ mutants. da – dorsal aorta, rda – recurved dorsal aorta, c – coelomic cavity, D – dorsal, V – ventral.

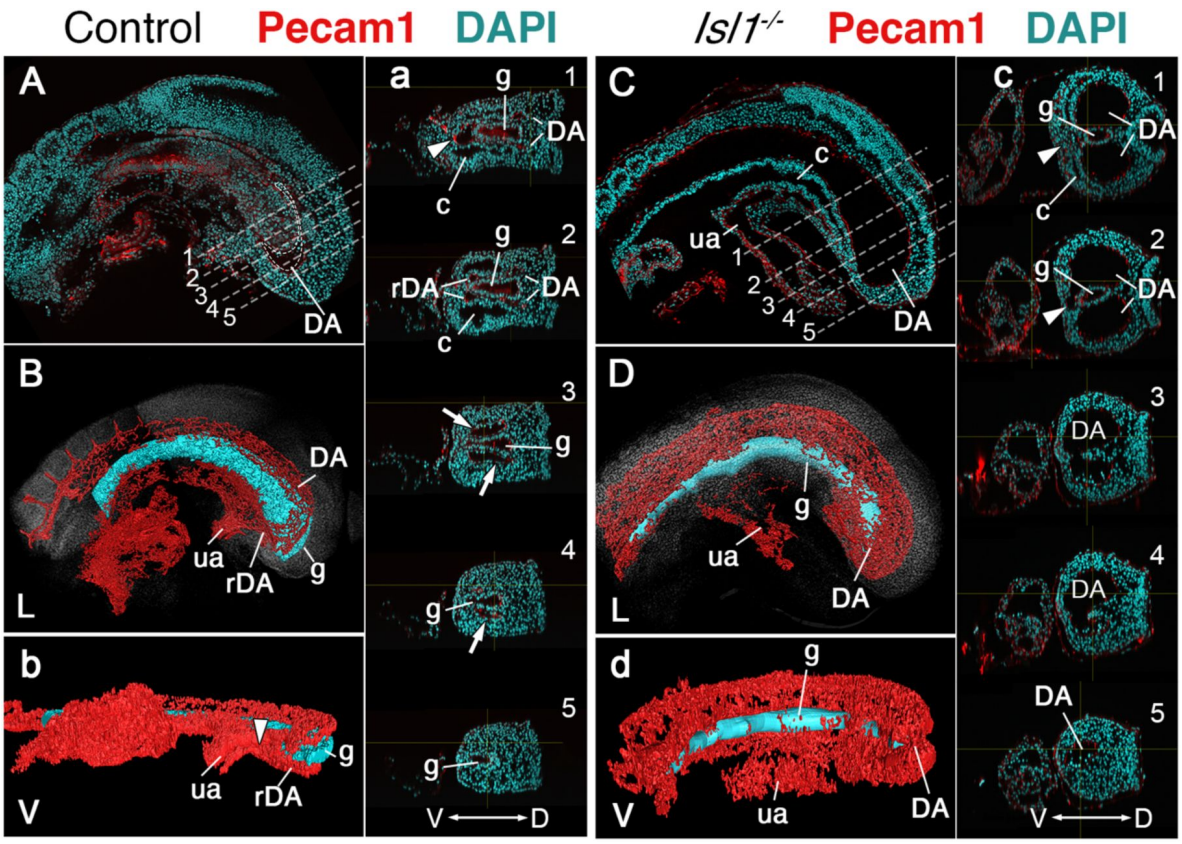

Figure 5.

Main vascular tree of the *Isl1*$^{-/-}$ embryos.

A, C. Wholemount immunostaining for Pecam1 (red) labelling endothelial cells in E9.5 control (A) and mutant (C) embryos. **a, c.** Optical transversal sections through regions marked by the dashed lines in A and C. **B, b, D, d.** 3D reconstruction of the main vascular tree (red) and the gut (cyan) of the immunostaining shown in (A, a, C, c). In the mutant recurved dorsal aorta (rDA) is underdeveloped and connection between dorsal aortae (DA) and the umbilical artery (ua) is established by a small vessel (white arrowhead in c1 and c2). Branches of DA are enlarged in the *Isl1*$^{-/-}$ and merge together at the posterior end and ventral to the gut (c3-5, d). D – dorsal, L – lateral, V – ventral, c – coelomic cavity, g – gut.

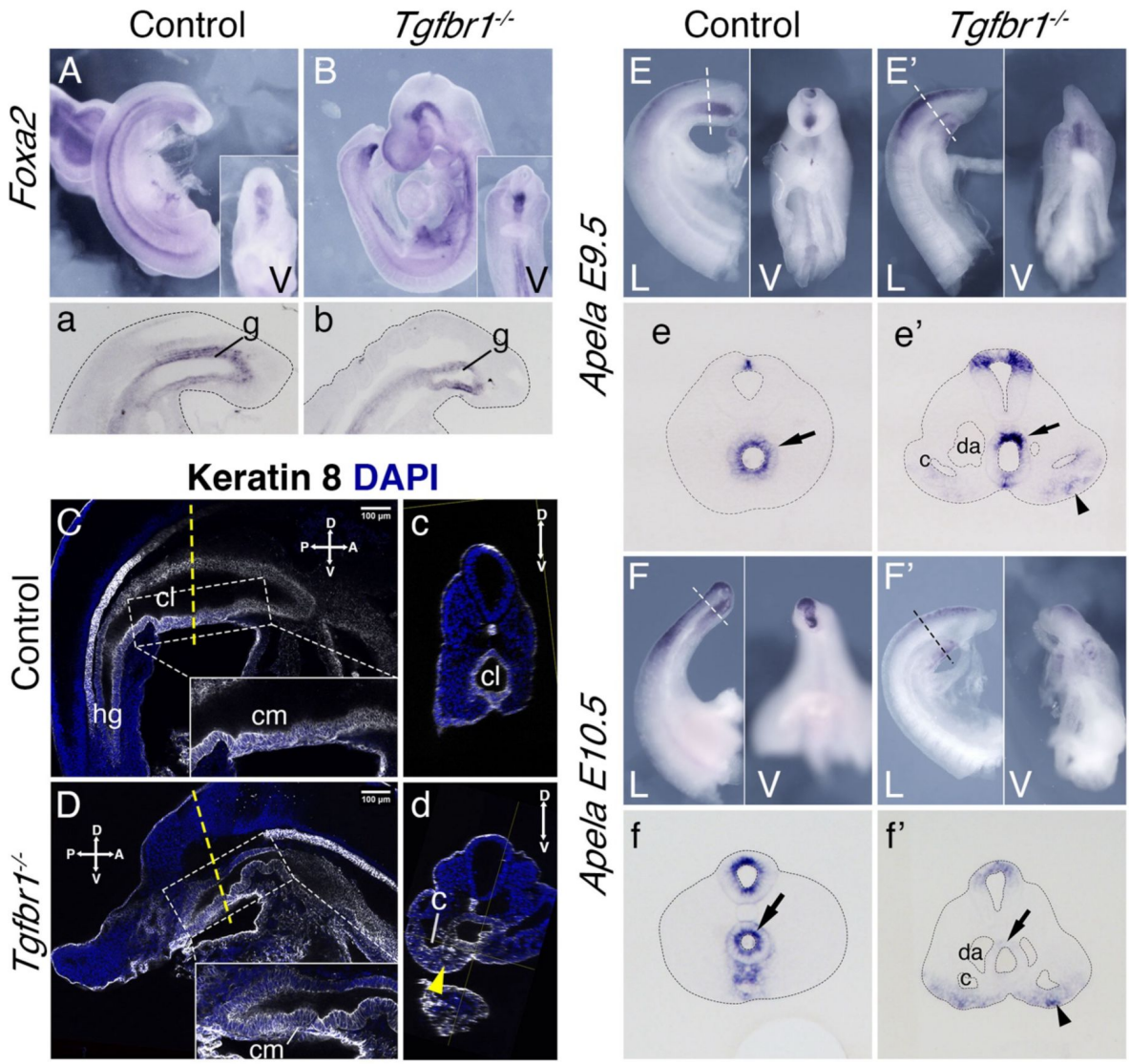

Figure 6.

Endoderm of the *Tgfbr1* KO.

A – b. Expression of *Foxa2* in E9.5 control (A, a) and *Tgfbr1* KO (B, b) embryos. a, b. show sagittal sections though the tail region. **C - d.** Keratin 8 staining of the cloaca region in the control (C,c) and *Tgfbr1*$^{-/-}$ (D,d) E10.5 embryos. *Tgfbr1*$^{-/-}$ do not initiate enlargement of the cloacal cavity. Insets show higher magnification of the cloacal membrane (cm). c and d show transversal optical sections marked by the dashed line in C and D. Yellow arrowhead in d shows keratin 8 staining in expanded LPM of the *Tgfbr1* mutant embryo. **E – e'.** *Apela* expression in the posterior region of the E9.5 control (E, e) and mutant (E', e') embryos. e and e' show transversal sections of regions marked by the dashed line in E and E'. **F–f'.** *Apela* expression in the posterior region of the E10.5 control (F, f) and mutant (F', f') embryos. f and f' show transversal sections of regions marked by the dashed line in F and F'. Black arrow – gut endoderm, black arrowhead – *Apela*-expressing cells in LPM of the mutant embryo. V–ventral, L–lateral, cl – cloaca, c – coelomic cavity, da – dorsal aorta, g – gut, hg – hindgut.

absence of *Tgfbr1* does not affect recruitment of visceral endodermal cells to the embryonic gut, and that the abnormal *Apela* patterns observed in *Tgfbr1* mutant embryos are unlikely to derive from misrouting of visceral endodermal cells.

Interestingly, while we observed a significant contribution of Afp-GFP-positive visceral endoderm cells to the embryonic endoderm of wild type embryos at E8.5 (**Fig. 7A,A'**), we could detect just a few cells in the tail gut of E9.5 embryos (**Fig. 7C-C''**) and virtually none at E10.5 (**Fig. 7E,E'**). This indicates that, while the visceral endoderm contributes significantly to the embryonic gut up to the region of the cloaca, as previously reported (Kwon et al., 2008), it is likely to play a minor role in the extension of the endodermal tube growing into the tail. The *Apela* expression patterns indicate that this gene is active in the newly generated endodermal tissues, becoming progressively downregulated after they are part of the gut tube (Hassan et al., 2010). The strong *Apela* expression restricted to the posterior portion of the endodermal tube within the developing tail, suggests that the tail gut grows from the addition of cells at the tip of this structure. Interestingly, analysis of the *T-str-creERT:ROSA26-R-gal* reporter activity upon tamoxifen administration at E8.0 showed the presence of β-galactosidase positive cells in the tail gut (**Fig. 3d**). A similar finding has also been independently reported using a different T-creERT strain (Anderson et al., 2013). Of note, more anterior regions of the gut, were negative for β-galactosidase under these conditions, despite the presence of labeled cells in adjacent mesodermal tissues (**Fig. 3c**). This suggests that the most caudal region of the gut tube grows through the addition of cells generated from a structure derived from the primitive streak located at the end of the growing tail. Consistent with this hypothesis, we observed an *Apela*-positive structure adjacent to the tip of the gut at the posterior end of the growing tail (Supplementary Fig. 7C). A similar structure was observed in embryos immunostained for Keratin 8 (**Fig. 8**; Supplementary Fig. 7A-b).

We further tested whether this *Apela* and Keratin 8-positive region at the tip of the tailbud contributes to the gut tube using a DiI-mediated cell tracing approach *ex vivo*. E9.5 embryos injected with DiI that showed no label in the gut tube just after injection (Supplementary Fig. 8 A-c3) were analyzed after 20 hours in culture (**Fig. 8E-h'** and Supplementary Fig. 8). In the three embryos that filled this criterium, DiI-positive cells were observed in the gut tube epithelium. Additionally, staining was observed in the surrounding mesenchyme and in the neural tube, possibly due to DiI labeling also becoming incorporated into the NMC population. Even considering the possible leakage of the DiI into the NMC compartment, the presence of DiI signal in the gut epithelium further supports the existence of a region at the tip of the tailbud able to generate cells that become incorporated into the tail gut.

Discussion

The transition from trunk to tail development involves major tissue reorganization affecting all germ layers. Formation of spinal cord and somitic mesoderm is maintained by the relocation of the neural-mesodermal competent cells from the caudal lateral epiblast CLE in the epiblast into the CNH in the tailbud through an incomplete EMT triggered by the concurrent activity of Tgfbr1 and Snai1 (Cambray and Wilson, 2007; Dias et al., 2020; Henrique et al., 2015; Wilson et al., 2009; Wymeersch et al., 2021, 2019). The progenitors of the lateral mesoderm, however, undergo a process of terminal differentiation resulting in the formation of the primordia of the hindlimb and of the external genitalia (Jurberg et al., 2013). Genetic analyses indicate that *Tgfbr1* signaling is both necessary and sufficient to activate the mechanisms regulating those terminal differentiation processes, as illustrated by their premature activation in transgenic gain of function experiments (Jurberg et al., 2013) and the absence of early markers for the primordia of the hindlimb or the GT in *Tgfbr1* null mutant embryos (Dias et al., 2020). Our data now show that the requirement of *Tgfbr1* encompasses the development of many other tissues

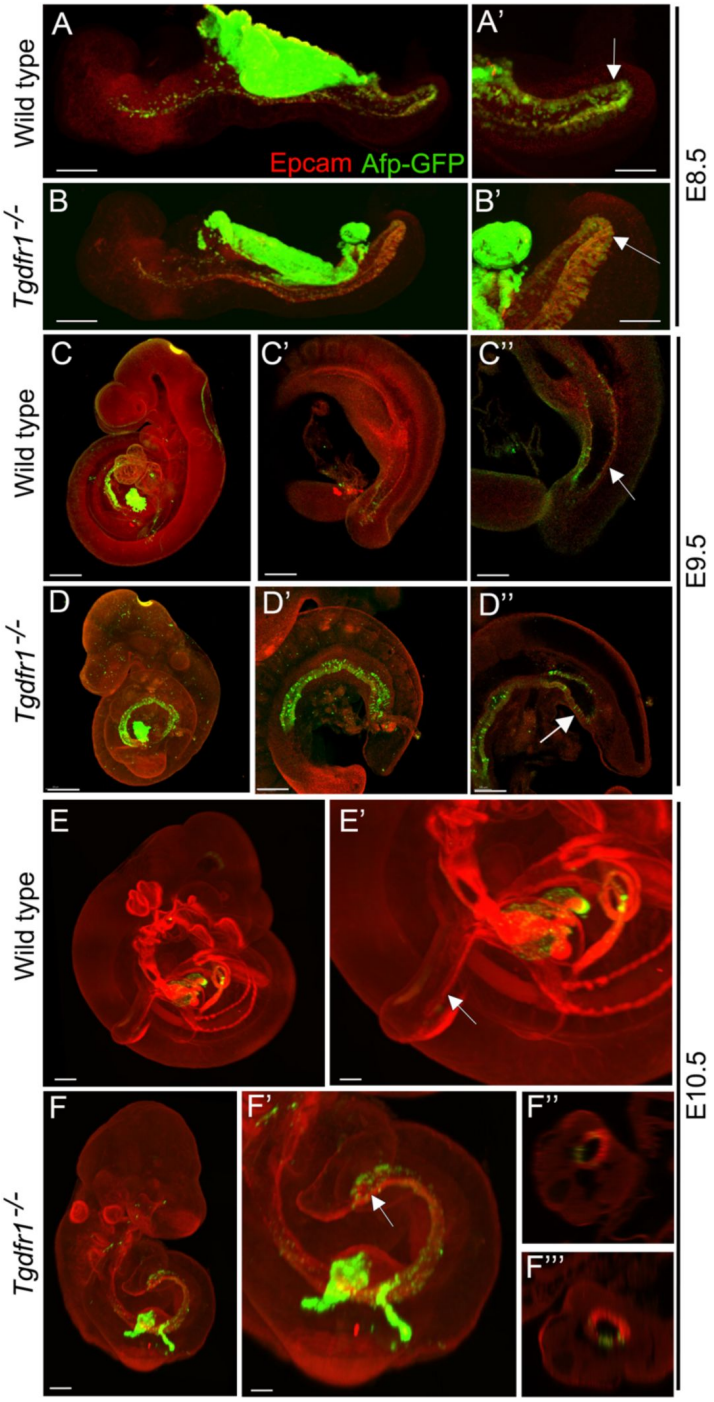

Figure 7.

Analysis of the contribution of the visceral endoderm to the embryonic gut.

GFP expression from the Afp-GFP transgenics was analyzed at E8.5 (A-B'), E9.5 (C-D'') or E10.5 (E-F''') in wild type (A, A', C-C'', E,E') or *Tgfbr1*$^{-/-}$ (B, B',D-D'', F-F''') embryos. C' and D' show a 3D image of the embryo, and C'' and D'' show transversal sections. F' and F'' show transversal sections through the caudal part of F'. The embryonic endoderm was labeled by immunofluorescence against Epcam. Arrows in A', B' indicate the hindgut; arrows in C'' and E' indicate the tail gut; arrows in D'' and F' indicate the cloacal membrane. Size bars: A, B: 200 µm; A', B': 100 µm; C, D: 300 µm; C', D': 200 µm; C'', D'': 150 µm; E: 300 µm; F: 200 µm; E': 150 µm; F': 100 µm.

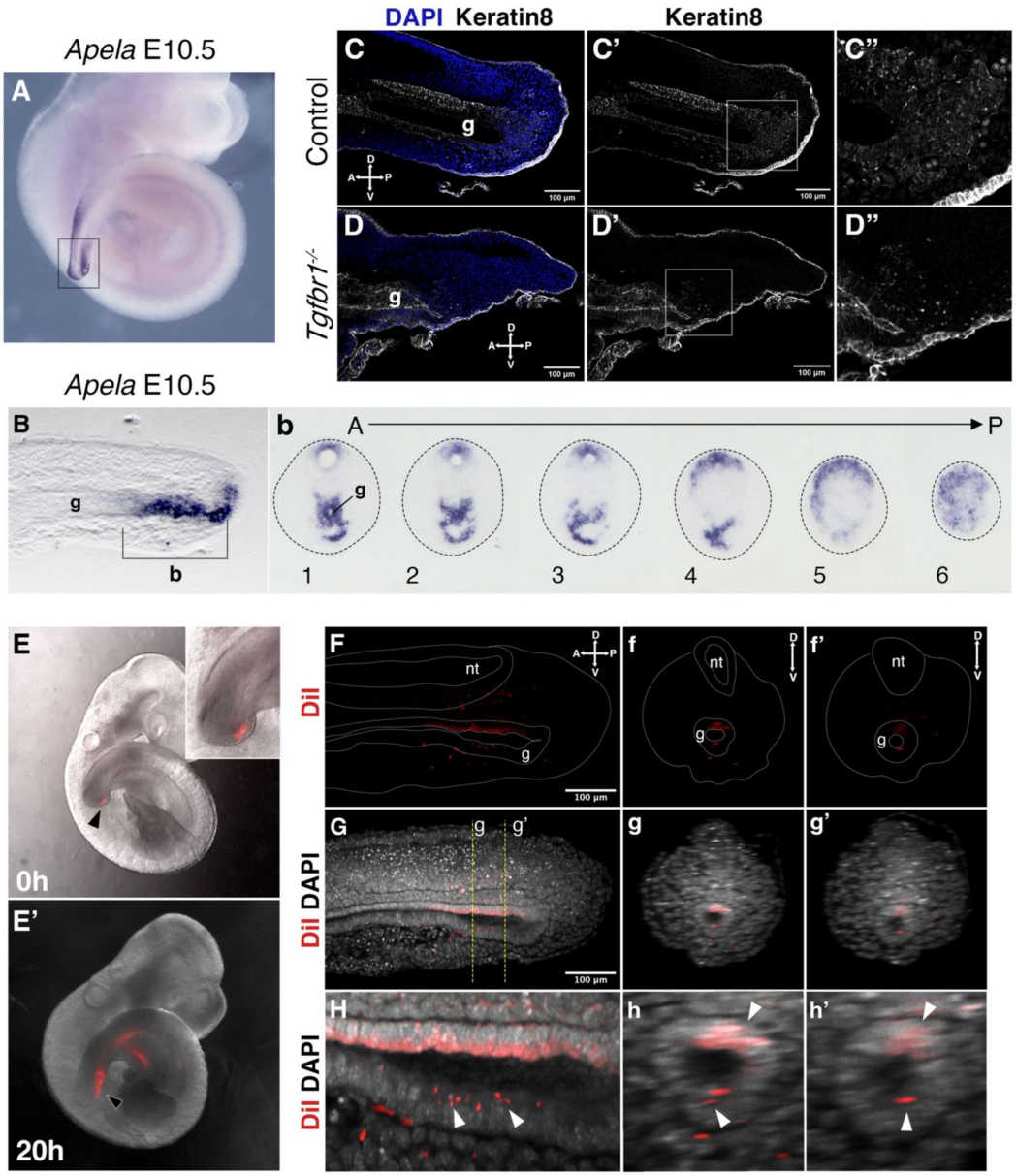

Figure 8.

Tail gut endoderm have contribution from the posterior pool of tailbud cells.

A. Whole mount *in situ* hybridization showing expression of *Apela* in E10.5 wild type embryo. **B.** Sagittal section through the region marked by rectangle in A shows presence of *Apela*-stained structure posterior to tail gut endoderm. **b.** Series of transversal sections though the *Apela*-expressing region posterior to the gut endoderm (marked by square bracket in B). **C-D''.** Sagittal optical sections through the tail region of the whole-mount immunostaining for Keratin 8 (white) in E10.5 control (C-C'') and *Tgfbr1*$^{-/-}$ (D-D'') embryos. Nuclei are shown in blue. Squares in C' and D' show the pool of epithelial cells posterior to the tail gut tube. This region coincides with newly formed endodermal cells expressing *Apela* shown in B, b. C''. D'' higher magnification of the region marked by square in C' and D'. A – anterior, P – posterior, g – gut. **E, E'**. Whole mount images of embryos injected with DiI in the Apela-positive region of the tail bud posterior to the gut endoderm, just after injection (E) or after 20 hours of incubation (E'). The magnification of the tail bud in the inset shows the absence of label in the gut tube. **F-h'.** Optical sections from two-photon images of the embryo in E' to show the presence of DiI cells in the gut tube. F-H show sagittal sections; f-h' show transverse sections. F-f'' show the DiI channel; tail, neural tube (nt) and gut (g) are outlined with a dashed line. G-g' show DiI and DAPI channels together. H-h' show magnification of DiI labeling in the gut tube (white arrowheads).

undergoing a morphological and functional reorganization during the trunk to tail transition, including the major vascular system and the embryonic endoderm. These observations place *Tgfbr1* as a master regulator of the trunk to tail transition.

An interesting conclusion from our work is the identification of the posterior PS/allantois as a candidate for the structure mediating the different *Tgfbr1*-dependent processes involving the lateral mesoderm and endoderm during the trunk to tail transition. Cell tracing experiments identified the posterior epiblast/PS as the region providing the cells building the trunk LPM (Wymeersch et al., 2016), being the posterior PS abutting the allantois also involved in organizing the recruitment of visceral endodermal cells to the embryonic gut tube (Rodriguez and Downs, 2017). The transition to tail development entails the fading of the epiblast and PS, as they become replaced by the tail bud as the main driver of axial extension. At this stage, the allantois also leaves its position at the posterior end of the embryo to occupy more anterior and ventral positions while organizing the connection between embryonic and extraembryonic structures (Arora and Papaioannou, 2012; Downs and Rodriguez, 2020). Gene expression analysis shows that genes involved in vascular morphogenesis are specifically expressed in the posterior epiblast/PS region (Wymeersch et al., 2019). Cell tracing experiments indicate that the posterior epiblast/PS, which lays down the LPM during trunk formation, generates the VLM posterior to the allantois during the trunk to tail transition (Wymeersch et al., 2016) and that these cells contribute to the primordium of the external genitalia later in development (Tschopp et al., 2014). The involvement of the PS in the formation of the VLM and genital primordia is also supported by our reporter data with the *T-str-creERT* transgenic line and *Isl1* cell lineage analyses (Yang et al., 2006). The absence of VLM in the *Tgfbr1* mutants indicates that signaling through this receptor is required to organize the proper switch of the posterior epiblast/PS from a trunk developmental mode, involving entering VLM fates. *Foxf1*, which is expressed in the posterior PS, maintains expression in the derivatives of this structure after the transition to tail development (Supplementary Fig. 7) (Astorga and Carlsson, 2007). We suggest that the strong and expanded *Foxf1* expression throughout the posterior end of the extended LPM of the *Tgfbr1* mutant embryos represents a molecular vestige of posterior PS that failed to form the VLM, and instead became trapped within mis-patterned LPM extending from the trunk. As the posterior PS is also thought to play a relevant role in the connection of the paired DAs with the allantois artery to link the embryonic and extraembryonic vascular systems (Downs and Rodriguez, 2020), defective posterior PS reorganization during the trunk to tail transition could explain the DA abnormalities observed in the *Tgfbr1* mutant embryos.

The embryonic tailgut has received little attention and mechanisms of its growth remain largely unknown. Analysis of *Tgfbr1*$^{-/-}$ embryos revealed that signaling through this receptor is essential for the development of the endodermal tube posterior to the cloacal plate and potentially the cloaca itself. *Apela* expression in wild type embryos is high in the newly formed endoderm, becoming downregulated as the endodermal tube differentiates (Hassan et al., 2010). The presence of the highest *Apela* levels in the posterior part of the tail gut at different embryonic stages (Hassan et al., 2010) suggests that this structure grows through the addition of new tissue at its posterior end. The low levels of *Apela* expression in the endoderm of the *Tgfbr1* mutants might thus indicate that this structure was generated earlier in development, during the phase of trunk extension. In addition, the presence of *Apela* signal mixed with the LPM suggests that new endodermal cells are still produced but failed to enter the gut, being instead mistargeted to the mesoderm. The absence of fluorescence signal in the mesodermal tissue of *Tgfbr1*$^{-/-}$*:Afp-GFP* embryos indicates that those cells are most likely not derived from the posterior visceral endoderm (Kwon et al., 2008). Interestingly, the similarities between the *Apela* and *Foxf1* expression in the posterior region of *Tgfbr1* mutant embryos suggest that their developmental history might be somehow linked. Given the role of the posterior PS abutting the allantois in the recruitment of visceral endodermal cells to the embryonic gut (Rodriguez and Downs, 2017), it is possible that tail gut growth is organized by a structure derived from a specific region of the posterior PS that enters the tail during the transition to tail development. The existence of a region

at the tip of the tailbud that feeds cells to the gut tube is supported by our DiI tracing experiment. Understanding the cellular identity and developmental potential of this region requires further investigation. In addition, the observation that the ROSA26 reporter labels the tail gut when activated by the *T-str-creERT* driver at the stage of the trunk to tail transition (Anderson et al., 2013) (**Fig. 3d**) is consistent with the involvement of the PS or a derivative of this structure in the formation of the gut tube posterior to the cloacal membrane. Were this the case, the transition of this PS-derived structure should be under *Tgfbr1* control.

Taken together, this work along with previous studies, suggests that the control of the trunk to tail transition by *Tgfbr1* entails two distinct, and apparently independent, components acting on two areas of the epiblast/PS. The first component involves a cooperation between *Tgfbr1* and *Snai1* to organize the relocation of NMC progenitors from the CLE to the CNH through a partial EMT (Dias et al., 2020). This component is also associated with the generation of the tail bud that replaces the epiblast/PS as the driver of axial elongation (Wilson et al., 2009; Wymeersch et al., 2021). The second component would target the posterior part of the epiblast/PS containing the progenitors for the lateral mesoderm as well as an organizing center for endodermal development (summarized in **Fig. 9**). Here, *Tgfbr1* activity triggers a combination of programs leading to the organization of the exit channels of the intestinal and urogenital systems, as well as the connection of the embryonic and extraembryonic circulation, and the formation of the hindlimbs and external genitalia. The finding that *Isl1* mutants exhibit many of the features observed in the lateral mesoderm and vascular system of *Tgfbr1* mutants, together with the absence of *Isl1* expression in *Tgfbr1* mutants (Dias et al., 2020) identifies *Isl1* as a key downstream mediator of the second component of *Tgfbr1* activity controlling the trunk to tail transition. Additional work will be required to elucidate the mechanisms regulating the fate and cell dynamics of the posterior epiblast/PS during the trunk to tail transition.

Acknowledgements

We would like to thank the members of the Mallo lab for continuous support at different stages of this project, the IGC mouse facility for their help with animal housing, and the Mouse Genetics Core Facility of Memorial Sloan Kettering Cancer Center for rederivation of the *Tgfbr1* mouse line.

Funding

This project was funded by Fundação para a Ciência e a Tecnologia (FCT) grants 2022.01629.PTDC to MM (DOI: 10.54499/2022.01629.PTDC), the PhD fellowship PD/BD/128437/2017 to AL and the research infrastructure Congento LISBOA-01-0145-FEDER-022170 to the animal facility, co-financed by Lisboa 2020/FEDER and FCT (Portugal). AKH and YYK are supported by the NIH (R01DK127821, R01HD094868, R01HD035455, and P30CA008748).

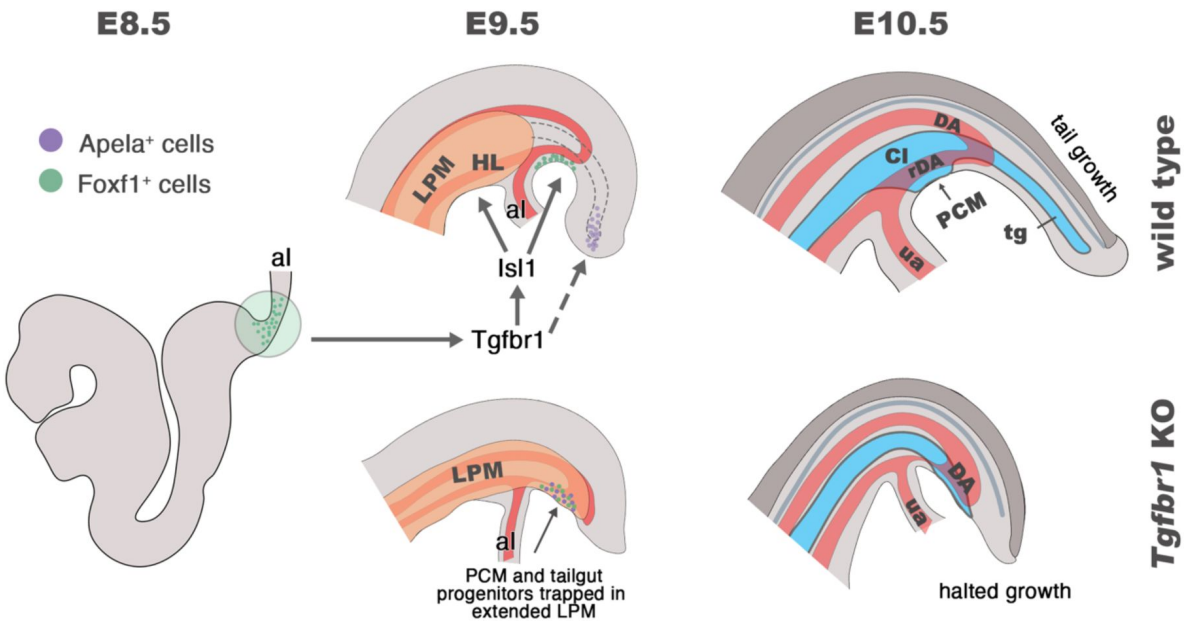

Figure 9.

Schematic representation of *Tgfbr1* activity on the posterior epiblast/PS region during the trunk to tail transition. At E8.5 embryo undergoes turning, associated with anterior relocation of the allantois along the ventral side of the embryo. In wild type embryos (top panel) *Tgfbr1* acts upstream of *Isl1*, which induces hindlimb (HL) formation from the somatic LPM, marking the posterior limit of this mesodermal compartment. Additionally, *Isl1* is involved in formation of the pericloacal mesenchyme (PCM), likely from the *Foxf1*$^{+}$ region in the posterior PS (shown in green), and in the development of the recurved dorsal aorta (rDA). Tailgut (tg) growth is, at least in part, supplied by the cells located in the tail bud (endodermal Apela^{+} cells are shown in purple). At E10.5 the trunk to tail transition is completed, resulting in the formation of the posterior trunk structures, including HL, cloaca (Cl), PCM and the connection of embryonic/extraembryonic (umbilical artery - ua) blood circulation via rDA. Tail growth continues generating neural tube (dark grey), presomitic mesoderm (not shown), and tg (blue). In the absence of *Tgfbr1* (bottom panel) *Isl1* is not activated, hindlimbs are not induced from the LPM, which, instead, keeps extending posteriorly. PCM and tg progenitor cells are misrouted and trapped in the posteriorly extended LPM. The rDA is underdeveloped. Development of *Tgfbr1* mutants is halted around E10.5.

References

Aires R, de Lemos L, Nóvoa A, Jurberg AD, Mascrez B, Duboule D, Mallo M. (2019) **Tail Bud Progenitor Activity Relies on a Network Comprising Gdf11, Lin28, and Hox13 Genes** *Dev Cell* **48**:383–395 https://doi.org/10.1016/j.devcel.2018.12.004

Anderson MJ, Naiche LA, Wilson CP, Elder C, Swing DA, Lewandoski M (2013) **TCreERT2, a Transgenic Mouse Line for Temporal Control of Cre-Mediated Recombination in Lineages Emerging from the Primitive Streak or Tail Bud** *PLoS One* **8** https://doi.org/10.1371/journal.pone.0062479

Andersson O, Reissmann E, Ibáñez CF (2006) **Growth differentiation factor 11 signals through the transforming growth factor-beta receptor ALK5 to regionalize the anterior-posterior axis** *EMBO Rep* **7**:831–837 https://doi.org/10.1038/sj.embor.7400752

Ang S-L, Wierda A, Wong D, Stevens KA, Cascio S, Rossant J, Zaret KS (1993) **The formation and maintenance of the definitive endoderm lineage in the mouse: involvement of HNF3/forkhead proteins** *Development* **119**:1301–1315

Arora R, Papaioannou VE (2012) **The murine allantois: A model system for the study of blood vessel formation** *Blood* https://doi.org/10.1182/blood-2012-03-390070

Astorga J, Carlsson P (2007) **Hedgehog induction of murine vasculogenesis is mediated by Foxf1 and Bmp4** *Development* **134**:3753–3761 https://doi.org/10.1242/dev.004432

Binagui-Casas A, Dias A, Guillot C, Metzis V, Saunders D (2021) **Building consensus in neuromesodermal research: Current advances and future biomedical perspectives** *Curr Opin Cell Biol* **73**:133–140 https://doi.org/10.1016/j.ceb.2021.08.003

Cai C-L, Liang X, Shi Y, Chu P-H, Pfaff SL, Chen J, Evans S (2003) **Isl1 identifies a cardiac progenitor population that proliferates prior to differentiation and contributes a majority of cells to the heart** *Developmental Cell* **5**:877–889

Cambray N, Wilson V (2007) **Two distinct sources for a population of maturing axial progenitors** *Development* **134**:2829–2840 https://doi.org/10.1242/dev.02877

Clements D, Taylor HC, Herrmann BG, Stott D (1996) **Distinct regulatory control of the Brachyury gene in axial and non-axial mesoderm suggests separation of mesoderm lineages early in mouse gastrulation** *Mech Dev* **56**:139–149

Cohn MJ (2011) **Development of the external genitalia: Conserved and divergent mechanisms of appendage patterning** *Developmental Dynamics* **240**:1108–1115 https://doi.org/10.1002/dvdy.22631

Davidson A (2008) **Mouse kidney development** *Stembook* https://doi.org/10.3824/stembook.1.34.1

Dias A, Lozovska A, Wymeersch FJ, Nóvoa A, Binagui-Casas A, Sobral D, Martins GG, Wilson V, Mallo M. (2020) **A Tgfbr1/Snai1-dependent developmental module at the core of vertebrate axial elongation** *Elife* **9** https://doi.org/10.7554/eLife.56615

Downs KM, Rodriguez AM (2020) **The mouse fetal-placental arterial connection: A paradigm involving the primitive streak and visceral endoderm with implications for human development** *Wiley Interdiscip Rev Dev Biol* https://doi.org/10.1002/wdev.362

Echelard Y, Epstein DJ, St-Jacques B, Shen L, Mohler J, McMahon JA, McMahon AP (1993) **Sonic hedgehog, a member of a family of putative signaling molecules, is implicated in the regulation of CNS polarity** *Cell* **75**:1417–1430 https://doi.org/10.1016/0092-8674(93)90627-3

Funayama N, Sato Y, Matsumoto K, Ogura T, Takahashi Y (1999) **Coelom formation: binary decision of the lateral plate mesoderm is controlled by the ectoderm** *Development* **126**:4129–4138

Hassan AS, Hou J, Wei W, Hoodless PA (2010) **Expression of two novel transcripts in the mouse definitive endoderm** *Gene Expression Patterns* **10**:127–134 https://doi.org/10.1016/j.gep.2010.02.001

Henrique D, Abranches E, Verrier L, Storey KG (2015) **Neuromesodermal progenitors and the making of the spinal cord** *Development* **142**:2864–2875 https://doi.org/10.1242/dev.119768

Hogan B, Beddington R, Constantini F, Lacy E. (1994) **Manipulating the mouse embryo: a laboratory manual** Cold Spring Harbour Laboratory Press

Huang YC, Chen F, Li X (2016) **Clarification of mammalian cloacal morphogenesis using high-resolution episcopic microscopy** *Dev Biol* **409**:106–113 https://doi.org/10.1016/j.ydbio.2015.10.018

Itou J, Kawakami H, Quach T, Osterwalder M, Evans SM, Zeller R, Kawakami Y (2012) **Islet1 regulates establishment of the posterior hindlimb field upstream of the Hand2-Shh morphoregulatory gene network in mouse embryos** *Development* **139**:1620–1629 https://doi.org/10.1242/dev.073056

Jurberg AD, Aires R, Varela-Lasheras I, Nóvoa A, Mallo M (2013) **Switching axial progenitors from producing trunk to tail tissues in vertebrate embryos** *Dev Cell* **25**:451–462 https://doi.org/10.1016/j.devcel.2013.05.009

Kawakami Y *et al.* (2011) **Islet1-mediated activation of the -catenin pathway is necessary for hindlimb initiation in mice** *Development* **138**:4465–4473 https://doi.org/10.1242/dev.065359

Kwon GS, Viotti M, Hadjantonakis AK (2008) **The Endoderm of the Mouse Embryo Arises by Dynamic Widespread Intercalation of Embryonic and Extraembryonic Lineages** *Dev Cell* **15**:509–520 https://doi.org/10.1016/j.devcel.2008.07.017

Mahlapuu M, Ormestad M, Enerbäck S, Carlsson P (2001) **The forkhead transcription factor Foxf1 is required for differentiation of extra-embryonic and lateral plate mesoderm** *Development* **128**:155–166

Matsubara Y *et al.* (2017) **Anatomical integration of the sacral-hindlimb unit coordinated by GDF11 underlies variation in hindlimb positioning in tetrapods** *Nat Ecol Evol* **1**:1392–1399 https://doi.org/10.1038/s41559-017-0247-y

Matsumaru D, Murashima A, Fukushima J, Senda S, Matsushita S, Nakagata N, Miyajima M, Yamada G (2015) **Systematic stereoscopic analyses for cloacal development: The origin of anorectal malformations** *Sci Rep* **5** https://doi.org/10.1038/srep13943

McPherron AC, Huynh T V, Lee S-J (2009) **Redundancy of myostatin and growth/differentiation factor 11 function** *BMC Dev Biol* **9** https://doi.org/10.1186/1471-213X-9-24

McPherron AC, Lawle AM, Lee S-J (1999) **Regulation of anterior/posterior patterning of the axial skeleton by growth/differentiation factor 11** *Nat Genet* **22**:260–264 https://doi.org/10.1038/10320

Nowotschin S, Hadjantonakis AK, Campbell K (2019) **The endoderm: A divergent cell lineage with many commonalities** *Development (Cambridge)* https://doi.org/10.1242/dev.150920

Prummel KD, Nieuwenhuize S, Mosimann C (2020) **The lateral plate mesoderm** *Development (Cambridge)* **147** https://doi.org/10.1242/dev.175059

Renier N, Wu Z, Simon DJ, Yang J, Ariel P, Tessier-Lavigne M (2014) **IDISCO: A simple, rapid method to immunolabel large tissue samples for volume imaging** *Cell* **159**:896–910 https://doi.org/10.1016/j.cell.2014.10.010

Rodriguez AM, Downs KM (2017) **Visceral endoderm and the primitive streak interact to build the fetal-placental interface of the mouse gastrula** *Dev Biol* **432**:98–124 https://doi.org/10.1016/j.ydbio.2017.08.026

Runck LA, Method A, Bischoff A, Levitt M, Penã A, Collins MH, Gupta A, Shanmukhappa S, Wells JM, Guasch G (2014) **Defining the molecular pathologies in cloaca malformation: Similarities between mouse and human** *DMM Disease Models and Mechanisms* **7**:483–493 https://doi.org/10.1242/dmm.014530

Soriano P (1999) **Generalized lacZ expression with the ROSA26 Cre reporter strain** *Nat Genet* **21**:70–71 https://doi.org/10.1038/5007

Srinivas S, Watanabe T, Lin C-S, William CM, Tanabe Y, Jessell TM, Costantini F (2001) **Cre reporter strains produced by targeted insertion of EYFP and ECFP into the ROSA26 locus** *BMC Dev Biol* **1** https://doi.org/10.1186/1471-213X-1-4

Steventon B, Martinez Arias A (2017) **Evo-engineering and the cellular and molecular origins of the vertebrate spinal cord** *Dev Biol* **432**:3–13 https://doi.org/10.1016/j.ydbio.2017.01.021

Tickle C (2015) **How the embryo makes a limb: Determination, polarity and identity** *J Anat* **227**:418–430 https://doi.org/10.1111/joa.12361

Tsakiridis A, Wilson V (2015) **Assessing the bipotency of in vitro-derived neuromesodermal progenitors** *F1000Res* **4** https://doi.org/10.12688/f1000research.6345.2

Tschopp P, Sherratt E, Sanger TJ, Groner AC, Ariel C, Hu JK, Pourquié O, Gros J, Tabin CJ (2014) **A relative shift in cloacal location repositions external genitalia in amniote evolution** *Nature* **516**:391–394 https://doi.org/10.1038/nature13819.A

Tsiairis CD, McMahon AP (2009) **An Hh-Dependent Pathway in Lateral Plate Mesoderm Enables the Generation of Left/Right Asymmetry** *Current Biology* **19**:1912–1917 https://doi.org/10.1016/j.cub.2009.09.057

Wilson V, Olivera-Martínez I, Storey KG (2009) **Stem cells, signals and vertebrate body axis extension** *Development* **136**:1591–1604 https://doi.org/10.1242/dev.039172

Wymeersch FJ, Huang Y, Blin G, Cambray N, Wilkie R, Wong FCK, Wilson V (2016) **Position-dependent plasticity of distinct progenitor types in the primitive streak** *Elife* **5** https://doi.org/10.7554/eLife.10042

Wymeersch FJ, Skylaki S, Huang Y, Watson JA, Economou C, Marek-Johnston C, Tomlinson SR, Wilson V (2019) **Transcriptionally dynamic progenitor populations organised around a stable niche drive axial patterning** *Development (Cambridge)* **146** https://doi.org/10.1242/dev.168161

Wymeersch FJ, Wilson V, Tsakiridis A (2021) **Understanding axial progenitor biology in vivo and in vitro** *Development* **148** https://doi.org/10.1242/dev.180612

Yamada G, Suzuki K, Haraguchi R, Miyagawa S, Satoh Y, Kamimura M, Nakagata N, Kataoka H, Kuroiwa A, Chen Y (2006) **Molecular genetic cascades for external genitalia formation: An emerging organogenesis program** *Developmental Dynamics* **235**:1738–1752 https://doi.org/10.1002/dvdy.20807

Yang L, Cai CL, Lin L, Qyang Y, Chung C, Monteiro RM, Mummery CL, Fishman GI, Cogen A, Evans S (2006) **Isl1 Cre reveals a common Bmp pathway in heart and limb development** *Development* **133**:1575–1585 https://doi.org/10.1242/dev.02322

Zakin L, Reversade B, Kuroda H, Lyons K, De Robertis E. (2005) **Sirenomelia in Bmp7 and Tsg compound mutant mice: requirement for Bmp signaling in the development of ventral posterior mesoderm** *Development* **132**:2489–2499

Author information

Anastasiia Lozovska[&]
Instituto Gulbenkian de Ciência, Oeiras, Portugal
ORCID iD: 0000-0002-9842-6450

[&]Present address: Department of Molecular Genetics and Microbiology, University of Florida, Gainesville, USA

Ana Casaca
Instituto Gulbenkian de Ciência, Oeiras, Portugal, Gulbenkian Instititute for Molecular Medicine, Lisboa, Portugal
ORCID iD: 0000-0002-0706-8038

Ana Nóvoa
Instituto Gulbenkian de Ciência, Oeiras, Portugal, Gulbenkian Instititute for Molecular Medicine, Lisboa, Portugal
ORCID iD: 0000-0002-5668-5630

Ying-Yi Kuo
Developmental Biology Program, Sloan Kettering Institute, Memorial Sloan Kettering Cancer Center, New York, USA

Arnon D Jurberg[#]
Instituto Gulbenkian de Ciência, Oeiras, Portugal
ORCID iD: 0000-0003-3541-998X

[#]Present address: Universidade Estácio de Sá (UNESA)/Instituto de Educação Médica (IDOMED), Rio de Janeiro/RJ, Brazil, and Laboratório de Animais Transgênicos, Universidade Federal do Rio de Janeiro (UFRJ), Rio de Janeiro/RJ, Brazil.

Gabriel G Martins
Instituto Gulbenkian de Ciência, Oeiras, Portugal, Gulbenkian Instititute for Molecular Medicine, Lisboa, Portugal

Anna-Katerina Hadjantonakis
Developmental Biology Program, Sloan Kettering Institute, Memorial Sloan Kettering Cancer Center, New York, USA
ORCID iD: 0000-0002-7580-5124

Moises Mallo
Instituto Gulbenkian de Ciência, Oeiras, Portugal, Gulbenkian Instititute for Molecular Medicine, Lisboa, Portugal
ORCID iD: 0000-0002-9744-0912

mallo@igc.gulbenkian.pt; moises.mallo@gimm.pt

Editors

Reviewing Editor
Sofia Araújo
University of Barcelona, Barcelona, Spain

Senior Editor
Sofia Araújo
University of Barcelona, Barcelona, Spain

Joint Public Review:

Previously, this group showed that Tgfbr1 regulates the reorganization of the epiblast and primitive streak into the chordo-neural hinge and tailbud during the trunk-to-tail transition. Gdf11 signaling plays a crucial role in orchestrating the transition from trunk to tail tissues in vertebrate embryos, including the reallocation of axial progenitors into the tailbud and Tgfbr1 plays a key role in mediating its signaling activity. Progenitors that contribute to the extension of the neural tube and paraxial mesoderm into the tail are located in this region. In this work, the authors show that Tgfbr1 also regulates the reorganization of the posterior primitive streak/base of allantois and the endoderm as well.

By analyzing the morphological phenotypes and marker gene expression in Tgfbr1 mutant mouse embryos, they show that it regulates the merger of somatic and splanchnic layers of the lateral plate mesoderm, the posterior streak derivative. They also present evidence suggesting that Tgfbr1 acts upstream of Isl1 (key effector of Gdf11 signaling for controlling differentiation of lateral mesoderm progenitors) and regulates the remodelling of the major blood vessels, the lateral plate mesoderm and endoderm associated with the trunk-to-tail transition. Through a detailed phenotypic analysis, the authors observed that, similarly to Isl1

mutants, the lack of Tgfbr1 in mouse embryos hinders the activation of hindlimb and external genitalia maker genes and results in a failure of lateral plate mesoderm layers to converge during tail development. As a result, they interpret that ventral lateral mesoderm, which generates the peri cloacal mesenchyme and genital tuberculum, fails to specify.

They also show defects in the morphogenesis of the dorsal aorta at the trunk/tail juncture, resulting in an aberrant embryonic/extraembryonic vascular connection. Endoderm reorganization defects following abnormal morphogenesis of the gut tube in the Tgfbr1 mutants cause failure of tailgut formation and cloacal enlargement. Thus, Tgfbr1 activity regulates the morphogenesis of the trunk/tail junction and the morphogenetic switch in all germ layers required for continuing post-anal tail development. Taken together with the previous studies, this work places Gdf11/8 - Tgfbr1 signaling at the pivot of trunk-to-tail transition and the authors speculate that critical signaling through Tgfbr1 occurs in the posterior-most part of the caudal epiblast, close to the allantois.

The data shown is solid with excellent embryology/developmental biology. This work demonstrates meticulous execution and is presented in a comprehensive and coherent manner. Although not completely novel, the results/conclusions add to the known function of Gdf11 signaling during the trunk-to-tail transition.

https://doi.org/10.7554/eLife.94290.2.sa1

Author response:

The following is the authors' response to the original reviews.

> ***Joint Public Review:***
>
> *Previously, this group showed that Tgfbr1 regulates the reorganization of the epiblast and primitive streak into the chordo-neural hinge and tailbud during the trunk-to-tail transition. Gdf11 signaling plays a crucial role in orchestrating the transition from trunk to tail tissues in vertebrate embryos, including the reallocation of axial progenitors into the tailbud and Tgfbr1 plays a key role in mediating its signaling activity. Progenitors that contribute to the extension of the neural tube and paraxial mesoderm into the tail are located in this region. In this work, the authors show that Tgfbr1 also regulates the reorganization of the posterior primitive streak/base of allantois and the endoderm as well.*
>
> *By analyzing the morphological phenotypes and marker gene expression in Tgfbr1 mutant mouse embryos, they show that it regulates the merger of somatic and splanchnic layers of the lateral plate mesoderm, the posterior streak derivative. They also present evidence suggesting that Tgfbr1 acts upstream of Isl1 (key effector of Gdf11 signaling for controlling differentiation of lateral mesoderm progenitors) and regulates the remodelling of the major blood vessels, the lateral plate mesoderm and endoderm associated with the trunk-to-tail transition. Through a detailed phenotypic analysis, the authors observed that, similarly to Isl1 mutants, the lack of Tgfbr1 in mouse embryos hinders the activation of hindlimb and external genitalia maker genes and results in a failure of lateral plate mesoderm layers to converge during tail development. As a result, they interpret that ventral lateral mesoderm, which generates the peri cloacal mesenchyme and genital tuberculum, fails to specify.*
>
> *They also show defects in the morphogenesis of the dorsal aorta at the trunk/tail juncture, resulting in an aberrant embryonic/extraembryonic vascular connection. Endoderm reorganization defects following abnormal morphogenesis of the gut tube in the Tgfbr1 mutants cause failure of tailgut formation and cloacal enlargement. Thus,*

> *Tgfbr1 activity regulates the morphogenesis of the trunk/tail junction and the morphogenetic switch in all germ layers required for continuing post-anal tail development. Taken together with the previous studies, this work places Gdf11/8 - Tgfbr1 signaling at the pivot of trunk-to-tail transition and the authors speculate that critical signaling through Tgfbr1 occurs in the posterior-most part of the caudal epiblast, close to the allantois.*
>
> *Strengths:*
>
> *The data shown is solid with excellent embryology/developmental biology. This work demonstrates meticulous execution and is presented in a comprehensive and coherent manner. Although not completely novel, the results/conclusions add to the known function of Gdf11 signaling during the trunk-to-tail transition.*
>
> *Weaknesses:*
>
> *The authors rely on the expression of a small number of key regulatory genes to interpret the developmental defects. The alternative possibilities remain to be ruled out thoroughly. The manuscript is also quite descriptive and would benefit from more focused highlighting of the novelty regarding the absence of Tgfbr1 in the mouse embryo. They should also strengthen some of their conclusions with more details in the results.*

Although we used a limited number of key regulatory genes to interpret the phenotype, these genes were carefully chosen to focus on specific processes involving the lateral mesoderm, its derivatives, and the endoderm. In addition to these markers, we included references to other relevant markers that were previously analyzed and initially led us to examine the lateral plate mesoderm and tail gut in Tgfbr1 mutants. To strengthen our analysis, we have now incorporated additional data to clarify specific phenotypes. For instance, in situ hybridization (ISH) for Shh further confirms abnormalities at the caudal end of the endoderm in mutant embryos, while no endodermal defects are observed in the trunk region. We also included an analysis of the intermediate mesoderm, which shows abnormalities at the same level as those found in the lateral plate mesoderm and endoderm of Tgfbr1 mutants.

It's important to note that using additional markers to assess the epiblast/primitive streak of Tgfbr1 mutants at E7.5–E8.5, as suggested by a reviewer, is unlikely to yield new insights. At these early stages, Tgfbr1 mutant embryos do not display observable phenotypes in the main body axis. Data in this manuscript already demonstrate the absence of abnormalities at this stage, as shown in Figure 3 and Supplementary Figure 6. Additionally, the expression of certain genes showing abnormalities when the embryo would enter tail development, in the trunk their expression remains unaffected, indicating that trunk extension is not significantly impacted by Tgfbr1 deficiency. While transcriptomic analysis of these Tgfbr1 mutants could provide interesting insights, it would be more appropriate to focus on later developmental stages, which would be beyond the scope of the current study.

The second major critique was that the manuscript is primarily descriptive. We disagree with this assessment. Several hypotheses were rigorously tested using genetic approaches, including Isl1 knockout experiments, cell tracing from the primitive streak with a newly generated Cre driver to activate a reporter from the ROSA26 locus, and assessment of extraembryonic endoderm fate in Tgfbr1 mutants by introducing the Afp-GFP transgene into the Tgfbr1 mutant background. Additionally, we conducted tracing analyses of tail bud cell contributions to the tail gut via DiI injection and embryo incubation. To address potential concerns regarding this experiment, we have included data showing the DiI position immediately after injection to confirm that it does not contact the tail gut. We also considered and accounted for potential DiI leakage into neuromesodermal progenitors to clarify the endodermal results.

Our genetic and DiI experiments were specifically designed to differentiate between alternative hypotheses and to confirm hypotheses generated from other analyses. Additionally, improvements in some of the imaging data have helped address remaining concerns.

> ***Reviewer #1 (Recommendations For The Authors):***
>
> *I have listed my suggestions as queries. The authors may perform experiments or clarify by editing the text to address them.*

The authors state on Page 11 and elsewhere that the ventral lateral mesoderm is absent in the Tgfbr1 mutant. What is the basis for this conclusion? Are there specific markers for PCM or GT primordium?

> *The specific marker of PCM and GT primordium is Isl1. The absence of this marker in the Tgfbr1 mutants is shown in (Dias et al, 2020). The reference is introduced in the manuscript.*

A schematic illustrating the VLM and the expression patterns of Tgfbr1, Gdf11, etc., would be helpful.

Characterization of Gdf11 expression has been previously reported (e.g. McPherron et al 1999, cited in our manuscript). It is expressed in the region containing of axial progenitors before the trunk to tail transition and not expressed in the VLM. As for Tgfbr1 expression is hard to detect, likely because it is ubiquitously expressed at low level. We include in this document some pictures of an ISH, including a control using the Tgfbr1 mutants to illustrate that the staining resembling background actually represents Tgfbr1 expression. If the reviewers find it important, we can also incorporate these data into the manuscript. Under these circumstances, we feel that a schematic might not be very informative.

Author response image 1.

Image showing an example of an ISH procedure with a probe against Tgfbr1, showing widespread and low expression. The lower picture shows a ventral view of a stained wild type E10.5 embryo.

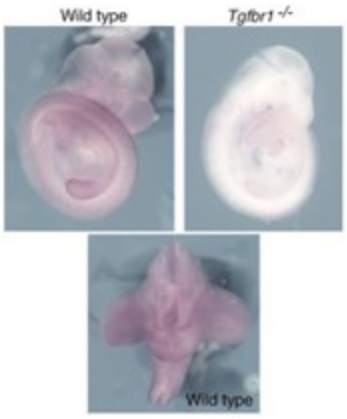

> *Foxf1+ cells in the 'extended LPM' of Tgfbr1 mutants suggest fate transformation, or does it indicate the misexpression of marker gene otherwise suppressed by Tgfbr1 activity? The authors suggest that Foxf1+ cells are VLM progenitors from posterior PS trapped in the extended LPM. Do they continue to express PS markers?*

The observation that both in wild type and Tgfbr1 mutant embryos Foxf1 expression in the trunk is restricted to the splanchnic LPM indicates that the absence of this marker in the somatic LPM is not the result of a suppression of its expression by Tgfbr1. In wild type embryos Foxf1 is also expressed in the posterior PS, regulated independently of its expression in the LPM (i.e. Shh-independent) and later in the pericloacal mesoderm (our supplementary figure 2). As Foxf1 expression in the posterior PS was not suppressed in the Tgfbr1 mutants, together with the absence of pericloacal mesoderm, we interpret that the Foxf1-positive cells in the two layers around the extended celomic cavity in the posterior end of the mutant embryos derived from the posterior PS, resulting from the absence of its normal progression through the embryonic tissues.

We did not find expression of PS markers giving rise to paraxial mesoderm, like Tbxt, further suggesting that those cells could derive from the restricted set of cells within the posterior PS that contribute to the pericloacal mesoderm

> *For example, the misexpression of Apela is interpreted as mis-localized endoderm cells. They show scattered Keratin 8 misexpression to support the interpretation. It would be more convincing if the authors tested the expression of other endoderm markers.*

As indicated in the manuscript, we suggest that these cells are endoderm progenitors (p. 13), like those present at the posterior end of the gut tube at E9.5 and E10.5, that are unable to incorporate into the gut tube. Apela is not a general endodermal marker: it is expressed in the foregut pocket and the nascent cells of the hindgut/tail gut, becoming down regulated as cells take typical endodermal signatures. The presence of ectopic Apela expression in the extended LPM of the mutant embryos might indeed indicate the presence of progenitors that failed to downregulate Apela resulting from the lack differentiation-associated downregulation. This would also implicate the absence of definitive endodermal markers.

> *The Nodal signaling pathway in the anterior PS drives endoderm development. It acts through Alk7. Does Tgfbr1 (Alk5) mutation impact endoderm development, in general? It isn't easy to assess this from the Foxa2 in situ RNA hybridization shown in Figures 6A and B. It would be helpful for the readers if the authors clarified this point.*

In the pictures shown in Figure 7D-D' it is already shown that the endoderm is mostly preserved until the region of the trunk to tail transition. The presence of a rather normal endoderm in the embryonic trunk can also be seen with Shh, a figure added as Supplementary Fig.5.

> ***Reviewer #2 (Recommendations For The Authors):***
>
> *The authors mention two interesting novel points which they should develop in the discussion, and probably also in the results.*
>
> *(1) The authors speculate about the possible involvement of the posterior PS as a mediator of Gdf11/Tgfbr1 signaling activity. However, as mentioned in the manuscript, their experiments do not allow regional sublocalization within the PS... Here it would be important to assess/discuss in more detail which progenitors respond to this signaling activity and when they do it. At the very least, the authors should provide high-resolution spatiotemporal data of the expression of Tgfbr1 in the PS.*

Tgfbr1 expression at this embryonic stage does not give clear differential patterns. The data reported for this expression in Andersson et al 2006 is very low quality and we have not been able to reproduce the reported pattern. On the contrary, all our efforts over the years provided a very general staining that could even be interpreted as background. When we

now included Tgfbr1 mutants as controls, it became clear that the ubiquitous and low level signal observed in wild type embryos indeed represent Tgfbr1 expression pattern: low level and ubiquitous. We are attaching a figure to this document illustrating these observations. If required, this can also be included in the manuscript as a supplementary figure.

> *Also, the work of Wymeersch et al., 2019 regarding the lateral plate mesoderm progenitors (LPMPs) should be referred to and discussed here.*

This was now added in the results (page 11) and in discussion (page 16).

> *For instance, are the LPMP transcriptomic differences detected between E7.5 and E8.5 caused by Tgfbr1 signaling activity? This question could be easily answered through a comparative bulk RNAseq analysis of the posterior-most region of the PS of mutant and WT embryos. The possible colocalization of Tgfb1 (Wymeersch et al., 2019) and Tgfbr1 in the LPMPs should also be addressed.*

We agree with the suggestion that RNA-seq in the posterior PS of WT and mutant embryos might be informative. However, it is very likely that within the proposed timeframe (E7.5 to E8.5) that there are no significant differences between the wild type and the Tgfbr1 mutant embryos because there is no apparent axial phenotype in Tgfbr1 mutant embryos before the trunk to tail transition. Therefore, at this stage, we think that this experiment is out of the scope of the present manuscript.

> *(2) The activity of Tgfbr1 during the trunk-to-tail transition is critical for the development of tail endodermal tissues. Here the authors suggest again the involvement of the posterior PS/allantois region, but a similar phenotype can also be observed for instance in the absence of Snai1 in the caudal epiblast (Dias et al., 2020)... It would be important to assess/discuss the origin of those morphogenetic problems in the gut. Is it due to the reallocation of NMC cells into the CNH? The tailbud-EMT process? LPMPs specification?... Regional mutations or gain of functions of Snai1 or Tgfbr1 in the caudal epiblast would help answer the question.*

The endodermal phenotype in the Snai1 mutants is different to that observed in the Tgfbr1 mutants. As can be observed in Figures 3, 4 and 5 of Dias et al. the absence of tailbud is replaced by a structure that extends the epiblast. As a consequence, the endoderm finishes at the base of that structure, even expanding to make a structure resembling the cloaca, which is different to what is seen in the Tgfbr1 mutants. In this case, the lack of tail gut is likely to result either from the lack of formation of the progenitors of the gut endoderm or from the dissociation of what would be the tail bud from the LPM. Actually, hindlimb/pericloacal mesoderm markers, like Tbx4, are preserved in the Snai1 mutant. As for the gain of function of Snai1 experiment, already reported also in Dias et al 2020, the destiny of these cells is not clear. The ISH for Foxa2 showed extra signals but as it is not an exclusive marker for endoderm it is not possible to know whether any of these signals correspond to endodermal tissues.

> *Regarding the development of tail endodermal tissues, the authors suggest that it occurs from a structure derived from the PS that is located posteriorly, in the tailbud, after the tip of the growing gut. This is an important and novel point as it suggests that the primordia of the endoderm is not wholly specified during gastrulation. So the observation should be well supported. How can Anastasiia et al. distinguish such "structure" from the actual developing gut? Does it have a distinct molecular signature or any morphological landmark that enables its separation from the actual gut? The data suggests that the region highlighted in Supplementary Figure 4Ab contains part of the actual gut tube (the same is suggested in Figure 5B). If the authors think otherwise,*

> *they must characterize that region of the tailbud by doing a thorough morphological and gene/protein expression analysis and assess its potency, via transplantation experiments. Also, the authors' claim mostly relies on the DiI experiments and those have three problems: #1 Anastasiia et al. assess "tail" endodermal growth at E9.5 when the correct stage to do it is after E10.5 (after tailbud formation). 2# Incongruencies, low number (only three embryos), and diversity in the results shown in Figure 8 and Supplementary Figure 4. For instance, despite similar staining at 0h, the extension and amount of DiI present in the gut tube after 20h varies significantly amongst the differently labeled embryos. A possible explanation lies in the abnormal leakiness of the DiI labelings and that is confirmed by the observations shown in Supplementary Figure 4M-O; the same for Supplementary Figure 4G, which shows a substantial amount of DiI in the neural tube. 3# The authors must provide high-quality data showing which tissues/regions were labelled at time 0h, including transversal and sagittal sections as they did for the 20h time-point. Additionally, it is important to re-orient the sagittal optical sections to a position that also shows the neural tube (like a mid-sagittal section) and include information concerning the AP/DV axis, as well as the location of the transversal optical sections in the sagittal image.*

As described in the reply to reviewer 1, Apela is expressed in the nascent tail gut endoderm but not in more anterior areas except for a foregut pocket, and becomes downregulated as the tube acquires endodermal signatures. Therefore, the structure to which the reviewer refers to might indeed represent a group of progenitors that extend the tail gut. And the observation that this property is observed only in the tail gut as it grows, already separates this region of the gut, which in the end do not contribute to mature organs, from more anterior areas of the endoderm (essentially anterior to the cloaca) that will become a relevant tissue of the intestinal organs. Our DiI labelling experiment was aimed to test whether this pool of cells contributes to the gut but does not allow to determine the nature of those cells, a question that will require further research (discussed on p. 17) and we think is beyond the scope of the present manuscript.

Regarding the labelling at E10.5, we agree that the tail bud in terms of NMCs is not completely formed, for example, at E9.5 the neuropore is not yet closed. However, we are more interested in regression of the epiblast, which is complete by E9.5. Injecting at E9.5 also has technical advantages for us, first, because in our hands earlier embryos grow better in culture, and second, because it is easier to inject in the tailbud at E9.5 because it is a little bit bigger than at E10.5. Therefore, injecting at E9.5 is less prone to technical artifacts due to injection inaccuracy and compromised growth in culture.

We agree that the injected DiI could also leak into NMPs, which might be located in the same area. However, while this could result in labeling of the neural tube, it would not affect the interpretation of the finding of labeled cells in the tail gut. Indeed, the presence of this label in the gut epithelium indicates the presence of progenitors in the injected region of the tail gut. We added some considerations of this the possible leakage into the results section of the manuscript (p. 15). We thank the reviewer for drawing our attention to this issue.

We also now provide high quality data showing labelled tissue at 0h in Supplementary figure 8A-c', higher magnification images in Fig. 8, and reoriented optical sections in Fig.6 and in Supplementary Fig. 7, including axis and location of the sections as suggested by the reviewer.

> *Minor concerns/comments:*
>
> *(1) The abstract is quite long, though this might be fine for this journal.*
>
> *(2) In relation to the comment on the abstract, the manuscript needs an initial Figure descrbing the events that are described in the introduction. Otherwise, the manuscript*

> *will only be accessible to mouse embryologists.*

We have a figure summarizing the results at the end of the manuscript, we think that including similar figure in the beginning might be redundant. What we could do, if required, is to include this type of schematic as a graphical abstract.

> *(3) The authors need to clarify what they mean when they use the following expressions "PS fate" and "fate of the posterior PS".*

I do not think that we have used such expressions. Indeed, they did not come out when we run a “find” in the word document. However, they would mean the tissue that would come out from them at later developmental stages.

> *(4) The assessment of Isl1 expression in Tgfbr1 mutant and transgenic mouse embryos would be better indicative of their molecular relationship than a comparative phenotypic analysis.*

These data have been reported in Dias et al 2020 and Jurberg et al 2013, both cited in the manuscript.

> *(5) The authors should explain or discuss what the upregulation of Foxa2 in the posterior end of Tgfbr1 mutants means.*

While an upregulation is apparent in the figure, looking at other pictures we cannot be sure of this being a significantly quantifiable up-regulation. We therefore removed the statement from the text.

> *(6) What happens to the intermediate mesoderm during the trunk-to-tail transition? Is Tgfbr1 involved in the regulation of its development?*

We have tested this using Pax2 and added the relevant data in Supplementary Fig. 1 and described in the results.

> *(7) The term "potential" should not be used during the description of DiI labeling experiments as this technique only assesses cell fate.*

Corrected

> *(8) Some figures lack AP/DV axis information (e.g. Figures 6, C, and D).*

Corrected

https://doi.org/10.7554/eLife.94290.2.sa0